154. Hydrogen Migration in Transition Metal Alkyne and Related Complexes

by **Jérôme Silvestre** and **Roald Hoffmann***

Department of Chemistry and Materials Science Center, Cornell University, Ithaca, NY 14853

(23.V.85)

The electronic and structural characteristics of the reaction interconverting a 1-alkyne complex into a vinylidene *via* a 1,2 hydrogen shift are examined. In a mononuclear system, initial slippage of the alkyne to an η^1 geometry is indicated. The subsequent step is shown to be analogous to the isomerization of a methylvinyl cation. We conclude that an alternative route involving a hydrido-acetylide species will be of much higher energy. A concerted shift in binuclear and trinuclear systems is ruled out, based on the loss of a strong bonding interaction between the alkyne and the metallic piece, in the transition state. In trinuclear systems, a mechanism for the isomerization is suggested involving prior oxidative addition of the C–H bond across a metal-metal bond. The metallic piece in this case assists the transformation. The discussion is extended to other reactions featuring hydrogen shifts; these include the intramolecular formation of a binuclear vinylidene from a 1,2-hydrido-acetylide complex, the isomerization of a binuclear μ-alkylidyne into a μ-vinyl geometry and the transfer of a bridging hydrogen onto a capping hydrocarbon fragment in trinuclear cluster complexes.

Transition metal elements have the remarkable ability to coordinate organic fragments or molecules. Beside the fascinating world of the structural chemistry thus generated, a crucial consequence of this ability to bind is essential modification of the organic species' chemical behavior. It is, of course, up to us, the chemists, to understand how these alterations operate. We would like ultimately (and ambitiously) to be able to monitor and tune these changes toward an obvious synthetic purpose.

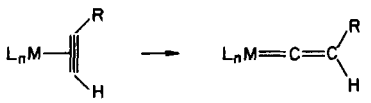

(1)

An attractive illustration of these considerations may be found in reaction (*1*) in which an acetylene-vinylidene rearrangement has occurred, mediated by, or centered on, a transition metal fragment ML_n. The transformation could be alternatively viewed as the isomerization of a transition metal alkyne into a vinylidene complex *via* a 1,2 H shift. This at first sight puzzling reaction has been mentioned several times in the recent literature, particularly with a mononuclear ML_n [1][1]) and is described as a way to obtain vinylidene complexes [4]. Intriguingly, binuclear frameworks appear to have no propensity for this type of reaction. In fact to the best of our knowledge only one case has been reported, with the mandatory presence of a halogen atom as the migrating group [5]. However, a somewhat related H shift was experimentally demonstrated by *Casey* and coworkers; the

[1]) For cases where η^2-alkyne was suggested as intermediates, see [2]. For cases where the vinylidene formation from an η^2-alkyne was suggested as a mechanistic step, see [3].

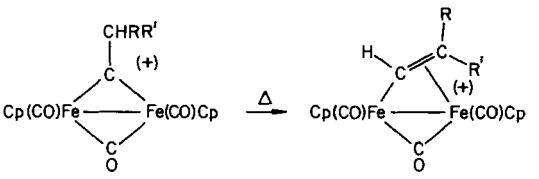

(2)

1 2

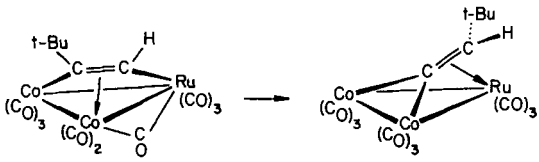

(3)

3 4

di-iron μ-alkylidyne **1** interconverts to the μ-vinyl complex **2** upon heating [6]. A beautiful example of an interconversion such as (*1*) on a trinuclear frame was recently published by *Vahrenkamp* [7], **3**→**4**. An X-ray structure determination of both the reactant and the product was made.

The role of the transition metal fragment in reactions such as (*1*), (*2*), and (*3*) is apparently not yet understood. In particular, for (*1*) and (*3*), it is not clear whether the formal 1,2 H shift proceeds in a concerted manner, similar to the hypothetical free-ligand isomerization, or *via* a more complex mechanism involving prior oxidative addition across the C–H bond, formation of a hydrido-acetylide intermediate, and subsequent migration to produce the vinylidene complex. The common denominator in all the transformations of type (*1*), (*2*), and (*3*) so far reported is the relatively mild thermal conditions required for the reactions to proceed. This certainly contrasts, for example, with the 'free'-acetylene→vinylidene rearrangement and makes the study of these isomerizations an interesting and challenging problem.

In this work, we investigate the geometrical and electronic features of the mechanism involved in reactions of the type (*1*), (*2*), and (*3*). The first section deals with an orbital analysis of the acetylene→vinylidene rearrangement free of transition metal complexation. Next, we bring in a mononuclear transition metal fragment and try to delineate the electronic features associated with three basic paths for (*1*). A discussion of why this reaction is reluctant to proceed in a binuclear case follows. The hypothetical intramolecular formation of a binuclear vinylidene complex from a hydrido-acetylide (*4*) is examined. This section concludes with an analysis of the rearrangement described in (*2*). Finally, we shall look in a more qualitative way at the role of the trinuclear frame in (*3*) and related reactions.

(4)

Our arguments and conclusions will be primarily based upon simple perturbation theory and both symmetry and overlap considerations supplemented by computations at the extended *Hückel* level. The geometrical and computational details are found in *Appendices 1* and *2*, respectively.

The $C_2H_2 \rightarrow CCH_2$ Isomerization. – There is in the literature an impressively large number of reports dealing with the acetylene-vinylidene rearrangement [8]. Numerous theoretical studies [9] have been carried out, primarily to determine the energy barrier associated with the process and to assess whether or not the vinylidene is a local minimum on the overall potential energy surface. Experimentally, there has been some evidence supporting the existence of a vinylidene species [8a] [10]. To assess the influence of a transition metal fragment on the isomerization reaction (*1*), we need to understand from an orbital point of view the electronic changes associated with the 1,2 H shift in the absence of the organometallic fragment. We shall go through this now.

The information one would like to get will be available from a *Walsh* diagram. It is necessary to know the transition state geometry, if a reasonable reaction path is to be computed. Despite the well-known deficiencies of our computational scheme in providing accurate bond lengths, we decided to optimize *locally* the transition state geometry in an expedient consistent manner. The C–C bond length was set at 1.40 Å and the three parameters r, α and ω, defined in **5**, varied independently within a relatively restricted range. For each pair (r, α), defining the location of the migrating hydrogen H* in polar coordinates relative to the midpoint of the C–C bond, 0, ω was optimized and the value of the energy plotted with respect to α and r [2]). This produces the piece of the potential energy surface displayed in **6**. The zero of energy is set at the lowest energy within the window shown. The energy contours are in kcal/mol and spaced by 2.0 kcal/mol. The

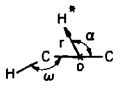

5

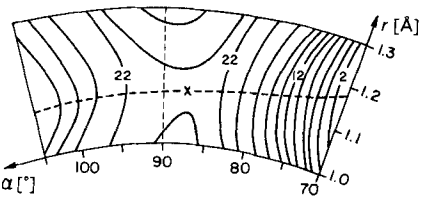

6

dashed line corresponds to the path the migrating H follows in the course of the shift. A careful look shows that the transition state, indicated by a crossed mark, is away from the line $\alpha = 90°$. In other words, at this point H* is closer to the carbon it is initially attached to than the incipient carbenic C-atom (1.30 Å *vs.* 1.36 Å). The angle ω optimizes at 169°. Over all, the geometry resulting from this crude procedure compares rather favorably with that obtained using a more rigorous treatment [8a] [9g].

The next step was to compute a *Walsh* diagram for the rearrangement along a path containing the transition state previously found. *Fig. 1* shows the essence of the orbital variations during the course of the isomerization. We choose the shift to occur within the

[2]) From now on, the hydrogen undergoing the migration will be starred in order to remove from the text any confusion involving the two different acetylene hydrogens.

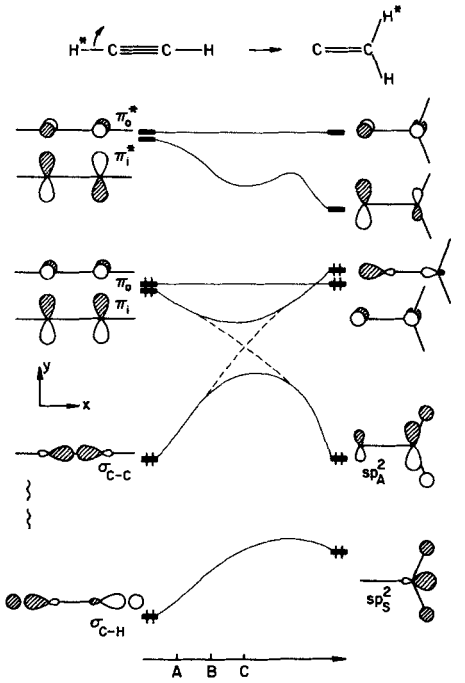

Fig. 1. *A* Walsh *diagram for the acetylene-vinylidene isomerization*

xy plane, the plane of the paper. The C–C axis lies along the *x* axis. At left, starting from the top of *Fig. 1*, are the two acetylene antibonding orbitals of π symmetry, π_i^* and π_o^*, the in-plane and out-of-plane components, respectively. Next, we find π_i and π_o, their bonding counterparts. Lower in energy, the C–C σ bond lies above the antisymmetric (with respect to the *yz* plane) combination of the C–H σ bonds. Left off the picture and further down is the symmetric combination.

Upon rotation and ultimate scission of the C–H* bond, orbitals of the same symmetry mix. Along the reaction, only the plane of the paper is maintained as an element of symmetry. Since the action takes place in this plane, the perpendicular π orbitals (π_o, π_o^*) are unaltered by the shift. The picture that emerges is relatively clear. The two orbitals of σ character rise in energy, due to the loss of bonding. The σ_{C-H} molecular orbital is most affected by the distortion but it is the higher lying C–C σ bond that ultimately sees its energy greatly increased, in a kind of avoided crossing. The in-plane π component is sandwiched between π_i^* which drops, and rising σ_{C-H}. Consequently, this MO remains almost flat. However, it picks up a lot of σ_{C-H} character and ultimately ends up as the σ lone pair of the vinylidene. This strong avoided crossing, (dashed line), between σ_{C-C} and π_i, converts the former into the antisymmetric (with respect to the *xz* plane) combination of the two C–H σ bonds, sp_A^2. From this picture it would appear that the C–C σ bond has disappeared. This, of course, is not true. The corresponding electron density is now located partly in the new HOMO (note the in-phase relationship between the two C atoms in it) and in the lowest occupied MO left off *Fig. 1*. From a more schematic and localized viewpoint, the essence of the H shift can be captured by looking at **7**. The C–H bond is broken heterolytically; the H atom migrates so as to bridge the

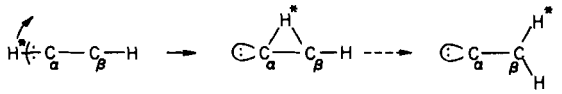

7

in-plane π obital. This picture has two implications: First, in terms of charges, the α C atom should grow negative and the H* migration might be characterized as protonic. Secondly, one should find an orbital in the transition state delocalized over C_α, C_β and H*, bonding over these three centers. This should represent the empty 1s orbital of the proton interacting with filled π_i in a bonding fashion. To check this last assertion and because we shall be interested in the topology of the orbitals at the transition state, snapshots were taken of σ_{C-C} and π_i in the early stage of the reaction, up to the transition state. The frames obtained are displayed in *Fig. 2*. From left to right one moves across points A, B and C in

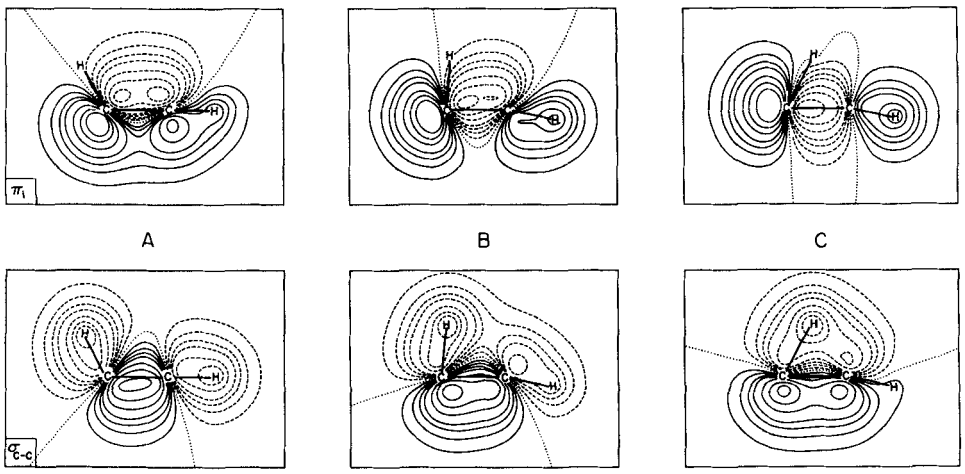

Fig. 2. Plots of molecular orbitals π_i (top) *and* σ_{C-C} (bottom) *at points* A, B *and* C *defined in* Fig. 1, *in the* x, y *plane.* Positive contours are solid lines; negative contours are dashed lines; the nodes are indicated by dotted lines. The absolute values of the contours are: 0.00, 0.035, 0.050, 0.075, 0.10, 0.15, 0.20, 0.25.

Fig. 1. At top is the morphological mutation of π_i; below that of σ_{C-C}. In geometry A, H* has already started to rotate. Look at σ_{C-C}: it clearly has some features of σ_{C-H}. The latter has already mixed with the former. The best way to visualize the avoided crossing between σ_{C-C} and π_i is to focus on the evolution of the shapes of the nodal surfaces going from A to C. Molecular orbital π_i at point A is clearly of π type. The nodal surface is bent a little because H* is off the C–C axis. In an ideal acetylene this node would lie along the axis. At point C, the same orbital exhibits a nodal surface roughly perpendicular to the axis. This matches essentially the nodal properties of σ_{C-C} at point A. Similarly, σ_{C-C} shows a nodal surface at point C closely related to that of a π bond, that is π_i. This orbital is the one previously anticipated, featuring a three-center delocalization between the pseudo-bridging H and the two C atoms. Going from A to C the two orbitals exchange their characteristics *via* the strong avoided crossing indicated by the dashed line in *Fig. 1*.

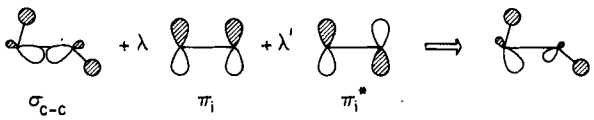

8

Simple perturbation theory[3]) helps to understand these transformations. Take for example σ_{C-C} at point B. Its shape results from the mixing of π_i and π_i^* into σ_{C-C}, in phase with respect to the migrating hydrogen. This is summarized in **8**. The orbital thus produced will *formally* end up as the vinylidene σ lone pair. We shall not dwell on the behavior of the empty orbitals. The antibonding combination of the broken C–H bond drops in energy and pushes down π_i^*, which in turn feels some repulsion from filled π_i. For future reference, it is sufficient to note that π_i^* correlates to the relatively low-lying LUMO of the vinylidene. This orbital is mainly concentrated on the carbenic C atom[4]) and obviously will serve as an excellent acceptor upon coordination of the vinylidene to a transition metal fragment.

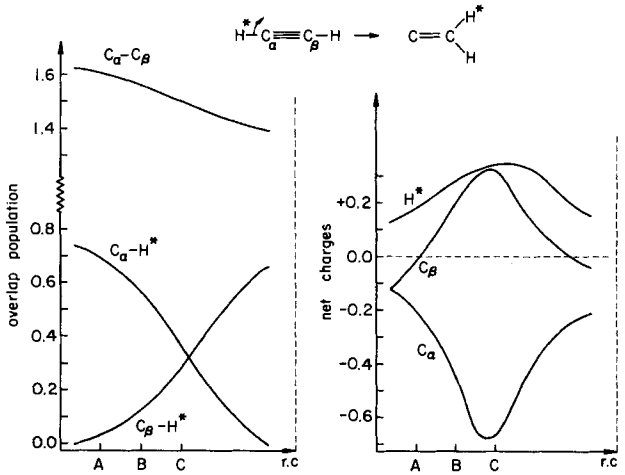

Fig. 3. Left: *plot of the overlap populations for the C_α–C_β, C_α–H* and C_β–H* bonds.* Right: *plot of the changes in the net charges of C_α, C_β and H**. In both plots, the reaction coordinate is the H shift taking the acetylene into the vinylidene.

Let us look at the evolution of both the overlap populations and the net charges during the course of the shift. The left side of *Fig. 3* shows the change in overlap population for the C–C bond, and the broken and the newly formed C–H bonds, along the chosen path. The C–C bond, despite the fixed bond length used throughout, exhibits a continuous decrease in strenght. The bond order is effectively reduced from 3 in the acetylene to 2 in the vinylidene.The other two curves are also without discontinuity and this implies that the path chosen for the *Walsh* diagram is a smooth and reasonable one. It

[3]) See for example [11].

[4]) This agrees with previous calculations [9e].

is amusing to notice that the curves corresponding to the broken and formed C–H bond cross in the neighborhood of point C, the transition state. The right-hand side of *Fig. 3* also deserves some comment. What is shown here is the evolution of the net charges on C_α, C_β and H*. The two C atoms behave in diametrically opposite fashion. There is a tremendous build-up of negative charge at C_α, the incipient bearer of the lone pair, whereas C_β grows appreciably positive. The slight electron density loss suffered by H* would lead us to think that it really migrates as a proton. This is certainly consistent with the simplified view depicted in **7**.

The final words in this section are devoted to some energetic considerations. Within our geometrical constraints, there is an activation energy of 76 kcal/mol to isomerizing the acetylene into the vinylidene. The latter is computed to lie 44 kcal/mol above the former in energy[5]). Based on *Hammond*'s postulate [12] the transition state should geometrically resemble the vinylidene. It is interesting that this resemblance is not quite obvious here[6]). Recall that H* is still closer to C_α than C_β at this point, as indicated in **6**. Not by much, though. Electronically, however, the transition state does resemble the vinylidene. Look at π_i at point C in *Fig. 2*: it is already the lone pair of CCH_2. Returning to the numerical results, it will be important to keep in mind that, in the free ligand, our computations overestimate the barrier for the 1, 2 H shift from the acetylene structure by $\sim$ 1.0 eV [9f].

The 1,2 H Shift Upon Coordination to a Mononuclear ML_n. – As was briefly discussed in the *Introduction*, the isomerization of an η^2-coordinated alkyne into a vinylidene complex has been mentioned several times in the literature. A sampling of the ML_n involved is shown in **9** [1a], **10** [1b], and **11** [1c]. We should also include here the results of *Chisholm* and *Clark* who, in the early seventies [13] showed that upon coordination of an alkyne to **12**, the carbonium ion **13** was generated *via* a hydride shift. It is important to

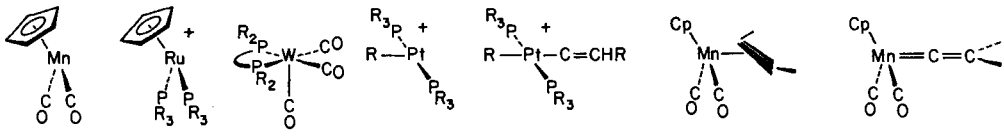

recognize the similarity between all the fragments drawn above. For instance, **9**, **10**, and **11** are of the d^6-ML_5 type. **12**, a T-shaped d^8-ML_3 piece, is isolobal to this triad [14]. It is clear also that all four fragments are isolobal with CH_3^+. We shall return shortly to the organic analogy.

Out of the four fragments **9**–**12**, we picked **9** to carry out the calculations. Later, a more economical model will be used. The questions to be dealt with in this section are: how can **14** proceed to **15**? What electronic factors influence the isomerization?

The electronic structure of both the reactant (**14**) and the product (**15**) has already been analyzed and may be found in [15]. Details will therefore be omitted and only the

---

[5]) These numbers lie within 10% of those obtained using *ab initio* calculations [9d] at the 4-31G level.

[6]) Calculations at the 6-31G* level agree with this conclusion [9d]. However, inclusion of *Moller-Plesset* correlation reverses this tendency [9b].

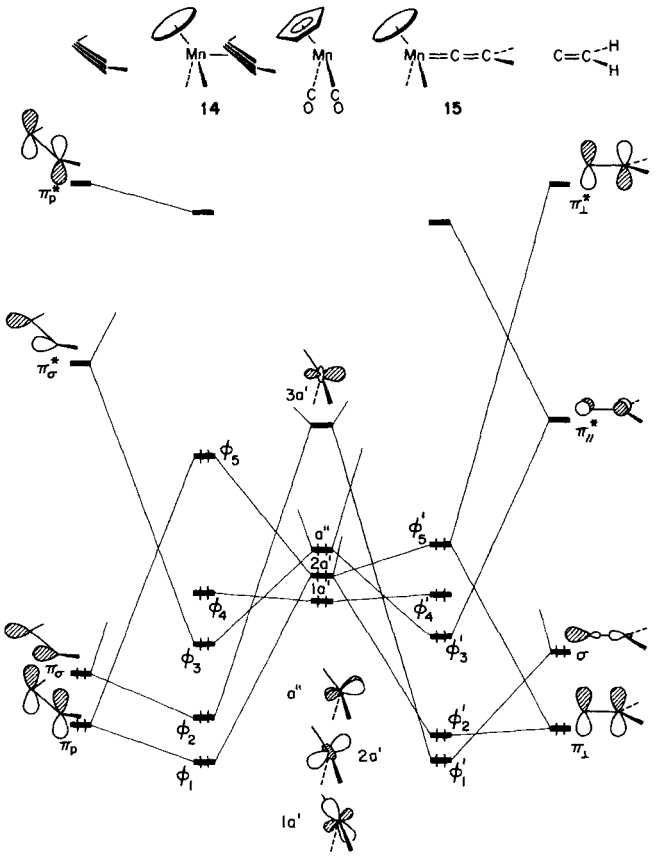

Fig. 4. *A comparative MO diagram between* **14** (left) *and* **15** (right) (see text)

salient features are outlined in the following. *Fig. 4* shows the essence of the bonding holding the two systems together. At center in *Fig. 4* are the valence orbitals of a $Mn(Cp)(CO)_2$ fragment. At the two extremes lie the orbitals of acetylene (left) and vinylidene (right). With the help of the usual fragment analysis [16], the molecular orbitals of **14** and **15** are constructed. This kind of side-by-side presentation has the merit of making eventual comparisons easier. The orbitals of the central unit are labelled according to the common C_s symmetry. Those of the acetylene are relabelled from *Fig. 1* taking into account whether they lead to σ or π bonding upon bending the H atoms away from the metal. The perpendicular or parallel subscript appended to the vinylidene orbitals refers to the CCH_2 plane. The two MO patterns produced upon interaction are strikingly similar. They illustrate perfectly the *Dewar-Chatt-Duncanson* model [17]. A filled ligand orbital interacts with an empty metal d orbital of cylindrical symmetry (π_σ and σ with 3a'), this is the forward donation. Back donation occurs *via* filled a'' on the metal into empty π_σ^* (C_2H_2 side) and π^* (CCH_2 side). In both systems, the fragment molecular orbital 1a' is a bystander. The general MO pattern for the two complexes is that of a d^6-ML_6 octahedral complex. We find the three highest occupied MO's ϕ_3, ϕ_4, ϕ_5

(and ϕ_3', ϕ_4', ϕ_5') having the characteristics of the t_{2g} set; similarly ϕ_2 and ϕ_1 (ϕ_2', ϕ_1') are metal-ligand bonding orbitals. In terms of energy, one computes the vinylidene complex **15** more stable than the acetylene one by 35 kcal/mol[7]). In other words, *upon coordination of a transition metal fragment the thermodynamic stability of the acetylene and the vinylidene is reversed.* This will have important consequences.

The reason for this state of affairs can be found to a first approximation in the HOMO of **14** and **15**. In the acetylene system, the HOMO is essentially the antibonding combination between 2a′ and π_p. In the vinylidene complex, the corresponding orbital is prevented from being too high in energy by secondary mixing of $\pi_\perp^*$. The HOMO therefore possesses more non-bonding character. The explanation for this difference is a symmetry-based one: in **14**, the mixing of antisymmetric π_p^* into the symmetric HOMO is nil. A further consequence of the high-lying HOMO in **14** is the inherent instability we would expect for such a complex. This turns out to be a well-established fact [19a][8]). Isostructural and isoelectronic compounds to **14**, but featuring a more electronegative (Group VI) transition metal are more stable[9]). Perhaps the reason lies in the HOMO, which in these Group VI complexes emerges at a lower energy, since 2a′ is lower to begin with.

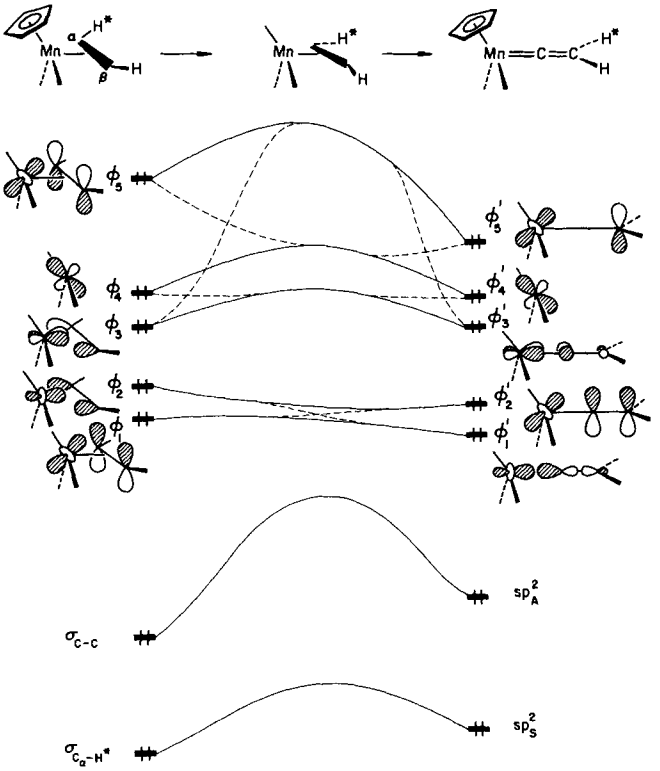

Fig. 5. *A* Walsh *diagram for a one-step synchronous* **14**-*to*-**15** *rearrangement*

[7]) This ordering was also found by others [18].

[8]) This compound was, however, reported stable when bound to a polymer [19b].

[9]) At least stable enough to grow crystals [20] and measure rotational barriers (see ref. 10 in [15a]).

Let us now turn to the isomerization reaction. We start by examining the possibility of a fully concerted reaction path. To put it another way, each of the bond-breaking and bond-forming processes is posited to occur at the same time. One can mimic such an idealized route by varying all the geometrical parameters which interconvert **14** and **15** in a synchronous manner. The activation energy associated with this path is high, 55 kcal/mol. A look at the corresponding *Walsh* diagram, sketched in *Fig. 5*, helps to understand why this is so. On the left of *Fig. 5* are the orbitals of **14**; at right, those of **15**. The nomenclature used for these molecular orbitals is identical to that introduced in *Figs. 1* and *4*.

During the course of the reaction, the plane of symmetry present in **14** and **15** is lost and much mixing takes place. A detailed examination of the orbital compositions, not presented here, makes clear the intended correlations. These are shown by dashed lines in *Fig. 5*. There are several contributions to the high computed barrier; both in the d block and in those orbitals centered on the hydrocarbon fragment. The concerted 1, 2 H shift which isomerizes **14** and **15** is not efficiently catalyzed by the metal. We were led to the conclusion that non-synchronous processes must be explored.

In the transformation **14**→**15**, one basically dismantled bonds; a C–H and a M–H one. The hint provided by the previous section is that one must break before the other. Which one? One may get this information by plotting a two-dimensional potential energy surface in which the two reaction coordinates measure to which extent the two bonds in question are broken. In **16**, we define these two parameters. X controls the shift of H* and

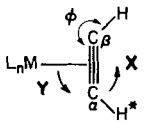

16

$L_nM \equiv Mn\,Cp(CO)_2$

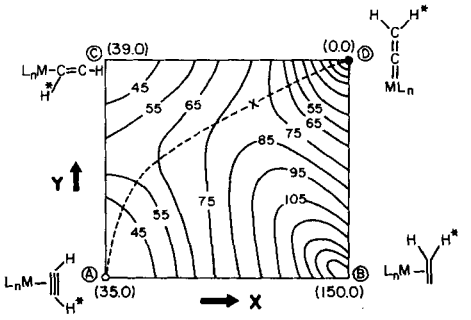

17

Y the pivotal motion of the ML_n unit around C_α. These two variables were incremented independently and again the angle ϕ (locating H with respect to the C–C axis) was optimized at each point. The corresponding energy surface was subsequently plotted in a X-*vs.*-Y diagram, **17**. The contours are in kcal/mol. The global minimum is point D, corresponding to the vinylidene complex **15**. As was previously stated, the acetylene complex lies some 35 kcal/mol higher in energy; it is the local minimum A. The disturbing feature of this surface lies in the absence of a channel between A and D. The reason is the unreasonably soft potential which would lead A to C. We think the low energy at point C as an artifact of the calculations. In fact, we encounter here a pathological deficiency of the one-electron theory used in this work. The hydrogen H* in C is unrealistically close to the metal (< 1.60 Å) and yet the calculations give no sign of a repulsion. One may

parenthetically notice that a path connecting A and D *via* a straight line would transit through a point lying ~ 50 kcal/mol above A. This matches our earlier results for a fully concerted route and suggests that the surface **17** bears some reality. Useful information can be extracted from **17**. In the early stages of the reaction, it is apparently easier to drift along the Y direction than to break the C–H bond (X). This certainly relates to the difference in strength between a M–C bond and a C–H bond. The dashed line in **17** tentatively represents a channel for the 1,2 H shift, if one allows oneself to disregard the misleadingly underestimated potential in the neighborhood of point C. The pseudo-transition state, (cross), lies at ~ 41 kcal/mol above the starting geometry, point A.

To fully understand and further exploit this idea, we shall now digress for a short while and concentrate on the organic analogue of the **14**→**15** rearrangement. Remembering the isolobal relationship between **9**–**12** and CH_3^+, the isomerization under study translates into the conversion **18**→**19**. The former is a corner-protonated cyclopropene,

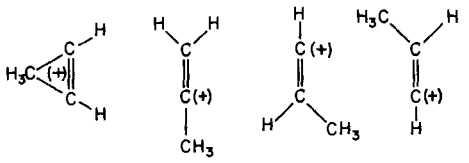

18 **19** **20** **21**

the latter one isomeric form of a methylvinyl cation. Alternatively, **18** can be visualized as a point on the potential energy surface which interconverts **20** and **21** *via* a CH_3 shift. In other words, starting with **18**, completion of the CH_3 shift leads to **20** (or **21**) which subsequently could be thought of as undergoing a H shift to produce **19**. We summarize pictorially these ideas on the right side of the *Chart*. At left is the sequence similar to that described above but now with CH_3^+ formally substituted by the isolobal $MnCp(CO)_2$ fragment, abbreviated ML_n here. What this analogy tells us is that on its way to the

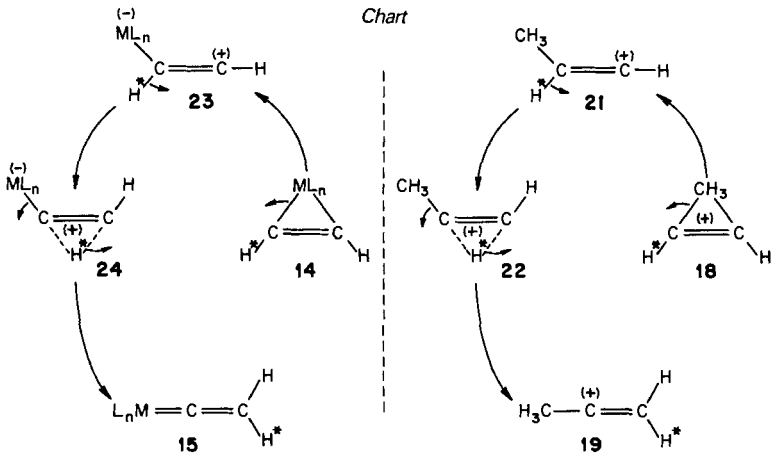

vinylidene complex **15**, **14** may very well transit an η^1-alkyne geometry, **23**. From a still different perspective, one might imagine the M–C bond is broken first, the C–H dissociation taking place only afterwards. This is precisely the conclusion we had reached from the potential energy surface shown in **17**. Remarkably, the isolobal concept could be carried one step further *via* the deprotonation analogy [14a]. By the substitution of first CH_3^+ and then CH_2 for $MnCp(CO)_2$, the **14**-to-**15** rearrangement becomes a cyclopropene-to-allene isomerization, **25**. Although this transformation has been observed [21] [22a, b][10]), it is likely to proceed by a radical-type of mechanism. We shall therefore preferentially make use of the analogy between ML_n and CH_3^+ according to the *Chart*.

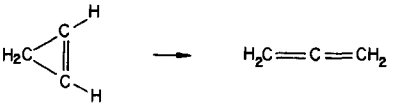

25

The 'organic' side of the *Chart* has received much attention in the last few years [23][11]), primarily in terms of the geometry and relative energy of the molecules involved. We shall not be concerned with these aspects here. In the following, we rather concentrate on the electronic changes associated with the sequence **21**→**22**→**19** and use the results as support for a comparison with what is happening during the transformation **23**→**24**→**15**.

From now on, the new starting point for the analysis is the analogue of **21** that is **23**, an η^1-alkyne complex, or alternatively an organometallic vinyl cation. We compute **23** to lie only 9 kcal/mol above **14**, the initial η^2-bound alkyne. Although it is somewhat difficult to trace this difference in terms of a *Walsh* diagram, we attribute the barrier to a loss of backbonding. Our next task was to recalculate a potential energy surface, now

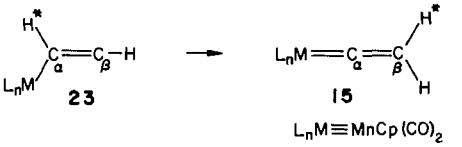

23 **15**

$L_nM \equiv MnCp(CO)_2$

going from **23** to **15**. Basically, the reaction coordinates are the same as those used for the construction of **17**. From left to right in *Fig. 6*, one monitors the shift of H* whereas from bottom to top, the pivotal motion of ML_n around the C–C axis is controlled. Also as before, the energies plotted in *Fig. 6* correspond to the best C_α–C_β–H angle. The contours are in kcal/mol. A similar problem to that encountered for **17** shows up: the ML_n unit has a tendency to 'catch up to' H*. However, the existence of a reaction channel is more apparent here. The dashed line emphasizes this point. The transition state (cross) lies $\sim$ 20 kcal/mol above the η^1-alkyne, which in turn is $\sim$ 44 kcal/mol higher in energy than the vinylidene complex. Adding the 9 kcal/mol required to slip the alkyne from an η^2 to an η^1 mode of binding, we compute an activation energy now of $\sim$ 29 kcal/mol for the isomerization **14**→**15**.

---

[10]) For the experimental and theoretical status of the C_3H_4 problem, see [22c].

[11]) For a more general account of vinyl cations, see [23c].

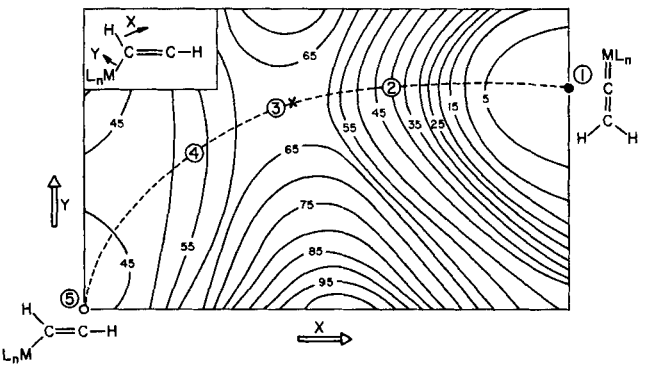

Fig. 6. A potential energy surface for the H shift taking **23** *into* **15**. The X coordinate monitors the H shift in an equally spaced 10-step process. The Y coordinate tunes the alignment of the ML_n unit along the C–C bond using an equally spaced 6-step process. The contours are equally spaced by 5.0 kcal/mol. The global minimum is the dark circle and is set to be the zero-energy point.

The reader will have noticed the five points scattered along the reaction path in *Fig. 6*. These serve as a basis for the following discussion of the geometrical and electronic changes occurring during the H shift.

To become better acquainted with the topological features of this reaction, we decided to plot the evolution of the atomic positions along the reaction path. This is done in *Fig. 7*. In this picture, the reader's eye is just above the plane where the action takes place. The location of the ML_n fragment is indicated by M. In the plane of the paper we plotted the cartesian coordinates of the atoms, at points ⑤–① of *Fig. 6*.

The striking feature of this plot is the difference in the pace at which the metal and H* move around C_α. In the first step ⑤ → ④, the metal has almost completed its rotation; the hydrogen however is still pretty well attached to C_α. The reasons for this were discussed earlier in the text. A further comment on this picture concerns the geometry at point ③, our transition state. The metal atom is almost colinear with the C–C axis. The migrating hydrogen, H*, is right above and close to the middle of this bond. One could therefore

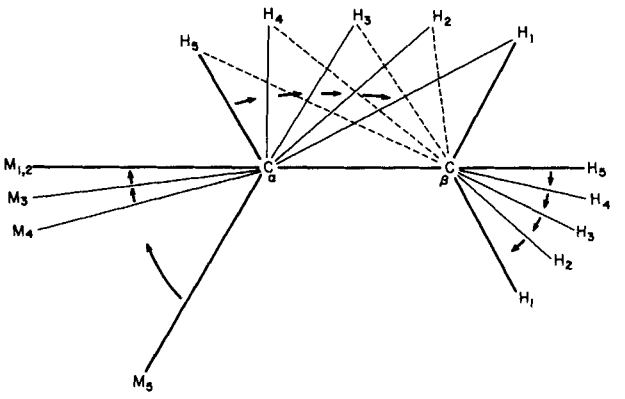

Fig. 7. *Topology of the H shift for the* **23**-*to*-**15** *transformation*. The numbers appended to each atom are the points defined in *Fig. 6* along the reaction channel.

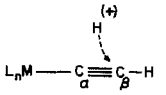

26

think of ③ as the transition state for the electrophilic addition of a proton to the triple bond of a terminal acetylide transition metal complex, **26**. Previous calculations as well as experimental facts [4] [24] support the idea of an ultimate addition to C_β. Conversely, cationic vinylidene complexes are known to undergo deprotonation in basic media [1b] [24c] [25].

Let us now turn our attention to the electronic changes associated with the H shift. The way the initial question of the acetylene-vinylidene isomerization assisted by a transition metal fragment was stated induced in our minds the idea of one specific mode of fragmentation: ML_n on one side, the hydrocarbon constituting the other piece. This is what we will call mode 1, **27a**. The organic analogy, however, led us to think of the process as a H shift in a 'methyl'-vinyl cation in which the CH_3 group is simply substituted by an isolobal transition metal fragment. This suggests another form of fragmentation,

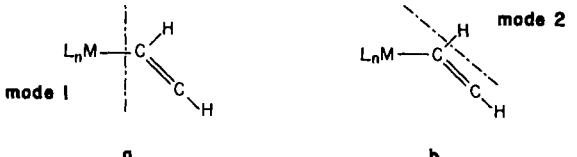

27

mode 2, **27b**. The hydrogen, alone, is one fragment and the rest of the molecule acts as the frame upon which the hydrogen migrates. The analysis that follows makes use of these two partition modes which, as we shall see, provide complementary information. At the bottom of *Fig. 8* is plotted the evolution of the overlap population of the bonds drastically altered in the reaction. The reaction coordinate is represented by the 5 points defined in *Fig. 6*. The gentle slope exhibited by all the curves is an indicator of a smooth and reasonable path. But there is more to be extracted from this information. The $M-C_\alpha$

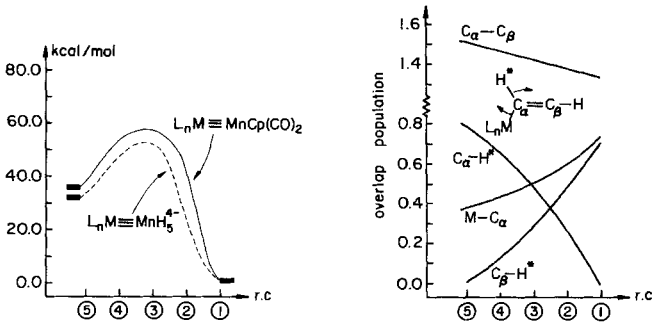

Fig. 8. Left: *Energy variation for interconversion of the η^1 structure into the vinylidene complex.* The solid (dashed) line refers to the ML_n being $MnCp(CO)_2$ (MnH_5^{4-}). Right: *Selected overlap populations for the* **23***-to-***15** *isomerization.*

overlap population grows steadily. This parallels the increase in formal bond order, from 1 to 2. It is furthermore encouraging to see that the bond-breaking and bond-forming curves (C_α–H*, C_β–H*) cross approximately at reaction waypoint ③, that is the chosen transition state. Finally, although there is no formal bond order change associated with the corresponding bond, the overlap population between C_α and C_β drops. A more efficient backbonding in the final vinylidene complex is the explanation. At the top of *Fig. 8* is shown the potential energy curve for the shift, with $ML_n \equiv MnCp(CO)_2$ and $ML_n \equiv MnH_5^{4-}$. Our intention is to show the similarity between the two cases. The energy scale is relative in each plot. The activation energy is basically the same, ~ 20 kcal/mol. In the remaining part of this section, we will therefore use the hydride model, **28**, to mimic

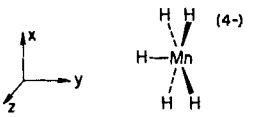

28

the ML_n fragment. Note the particular orientation of the H atoms. The one in the plane of the paper plus the two above the *xy* plane serve as substitutes for the cyclopentadienyl ring. The hydrocarbon fragment remains in the *xy* plane at all stages of the reaction. The four negative charges are adjusted to keep the metal atom in a d^6 configuration.

Not much insight into the influence of ML_n upon the shift is gained from a *Walsh* diagram. It is more rewarding to look at a fragment molecular orbital diagram, in mode 1, at the transition state. The picture is that schematically shown in *Fig. 9*. At left are the

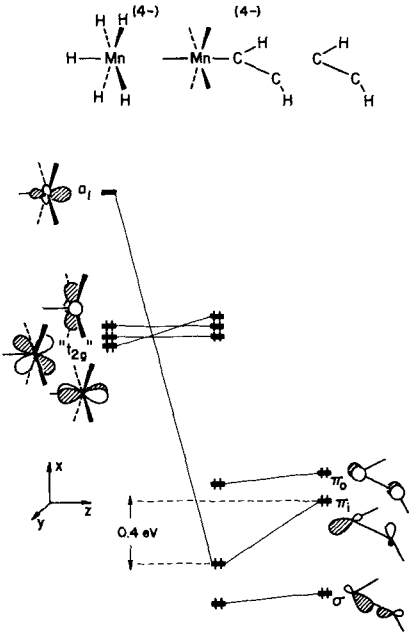

Fig. 9. *An interaction diagram at the transition state* ③ *defined in* Fig. 6, *in the reaction* **23**→**15**

valence orbitals of the C_{4v} ML_5 unit, **28**. The way these are constructed may be found, with details, in [14b] [26]. In short, take the three-below-two pattern of an octahedral complex, remove one ligand in the z direction and the z^2 orbital of the e_g set will come down to become the low-lying and strongly hybridized a_1 orbital of cylindrical symmetry shown in *Fig. 9*. The t_{2g} set is unaltered and houses the 6 electrons of a d^6 fragment. On the right-hand side of *Fig. 9*, are shown the orbitals of the hydrocarbon fragment, in the geometry obtained at point ③ of *Fig. 6*. We included here the two π components, π_o and π_i, plus the lower-lying σ orbital pushed up in energy by the distortion. Orbital π_i is severely deformed and its shape resembles pretty much that between point B and C of *Fig. 2*. The important point is its well-defined σ character, pointing towards the metal atom. Upon interaction orbitals of the same symmetry mix. The reader will have noticed that going from ML_n = $MnCp(CO)_2$ to the hydride model, we have gained a mirror plane of symmetry, namely xz. This certainly makes the analysis easier. The pseudo-t_{2g} set remains approximately non-bonding, d_{yz} being hardly destabilized by π_o. The low-lying σ orbital does not play a significant role, both for overlap and energy gap reasons. The vital interaction is that between empty a_1 on the metal and filled π_i. The overlap is large (0.30) and the outcome is the stabilization of π_i by 0.4 eV. This translates into a *net stabilization* of the hydrocarbon fragment at this geometry by 18.5 kcal/mol.

Let us now turn to the alternative fragmentation, mode 2 in **27**, and see how far the analogy with the methylvinyl cation can be pushed. The focus is then on the migrating hydrogen. We first build up the bonding in the η^1-geometries, **21** and **23**, by interacting an empty hydrogen 1s orbital, with acetylenic **29** and **30**. The resulting molecular orbital patterns are shown in *Fig. 10*. In the center lies the hydrogen s orbital. It interacts on the

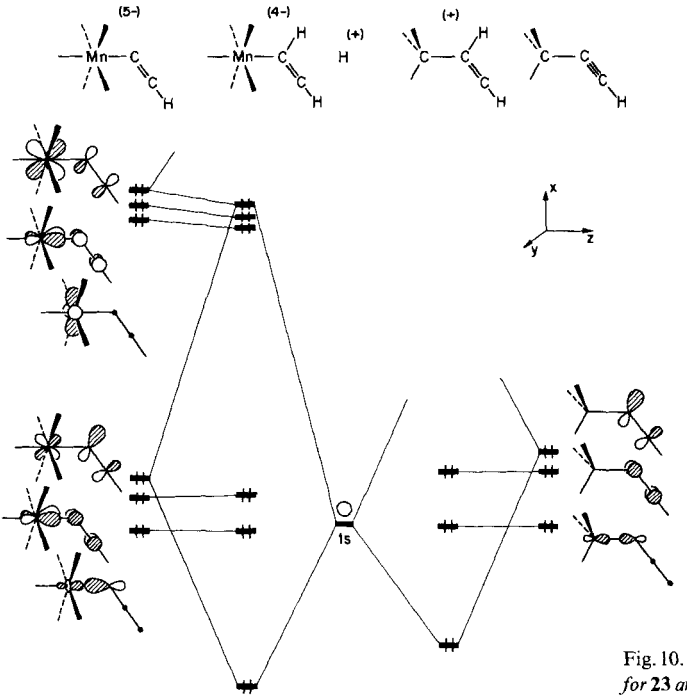

Fig. 10. *An interaction diagram for* **23** *and* **21**, *in mode 2* (see text)

29 **30**

left with the valence orbitals of **29**, on the right with those of **30**. Notice the very close orbital relationship between these two fragments. Both show a C_α-substituent σ bond; this is the lowest orbital on each side. Next is the out of plane π combination and then a filled sp^2 hybrid pointed towards the incoming hydrogen. Of course, there is no equivalent for the t_{2g} set on the pure organic fragment. When the hydrogen is allowed to interact, the expected C–H bond is created in both cases. The MO patterns for **21** and **23** are strikingly similar. The t_{2g} set in **29** is, however, not totally free of interaction. This is especially so for the d_{xz} orbital. One of its lobes, (in the $x > 0, z > 0$ quadrant) does feel the presence of the hydrogen. As a result d_{xz} mixes into the in-phase and out-of-phase combinations generated by the sp^2 hybrid and the hydrogen s orbital. To put it in another way, the hydrogen may be thought of having a slight tendency to attach the *metal* instead of C_α, *via* this d_{xz} orbital. We approach here the reason for the soft potential encountered in the surface of *Fig. 6*, where the hydrogen gets too close to the metal. We will see that the effect may be enhanced by an appropriate distortion of the metal-C_α–C_β backbone, ultimately leading to the oxidative addition product. In the geometry presently under consideration, it is important to realize the impossibility of the hydrogen entering a symmetrical bridging position between M and C_α. The nodal surface between the two atoms in d_{xz} works against that.

So far, so good. As could have been anticipated, the analogy between the electronic structure of the reactant, **23** and its organic *alter ego*, **21**, holds well. To follow the electronic changes during the shift, we still use the set of points, ⑤ to ① defined in *Fig. 6*, for both systems. An objection to this could have been that the transition state for the isomerization of the 2-propenyl cation to the 1-propenyl cation might not resemble the geometry at point ③. However, the computation of the energy curve for the organic rearrangement *via* point ③ shows the 2-propenyl cation to lie 11 kcal/mol above the 1-propenyl isomer with an associated activation energy of 25 kcal/mol. Again, these numbers agree with previous calculations carried out within a STO-3G or 4-31G parameterization [23a]. The match between the results of the calculations is in other ways not quite so good, since at the 6-31G* level a very tiny barrier is predicted to isomerizing the 2-propenyl cation into the 1-propenyl isomer. Our calculations, just as in the case of the acetylene-to-vinylidene rearrangement, overestimate the barrier. For the simple comparisons we wish to make we think that the use of the same path for both systems is still an allowable strategy.

Fig. 11 shows the evolution of the net charges on C_α and C_β and the migrating hydrogen during the course of the shift. Two features are interesting. First, C_α grows positive but certainly much more in the pure hydrocarbon. The excellent backbonding from the metal into the LUMO of the vinylidene (centered on C_α, as discussed earlier) is responsible for this. Also, H* becomes positive, although not dramatically. This supports the tendency of H* to shift as a proton rather than a hydride. A point must be made here. If both C_α and H* lose electron density where does that density go? The answer is: part of it onto the metal, but most of it goes to C_β, which then is ready to accept the incoming

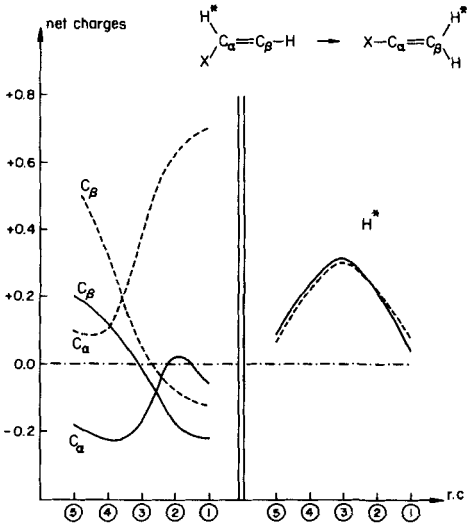

Fig. 11. *Net charges for the* **23**-*to*-**15** *and* **21**-*to*-**19** *isomerizations.* The solid (dashed) line refers to X being MnH_5^{4-} (CH_3^+).

protonic hydrogen. Note in *Fig. 11* that C_β ends up slightly more negative than C_α. This agrees with the idea of an electrophilic attack at the β site in vinylidene complexes. Second, in relation to the validity of the analogy suggested in the *Chart*, is the similarity[12]) of the results of the two types of substituents, ML_n on one hand, CH_3^+ on the other. Whether one has a CH_3 group or an isolobal transition metal fragment, the 1,2 H shift occurs in a similar manner. This statement is further supported by the results shown in *Fig. 12*. Here, we plot the reduced overlap population between the hydrogen and the rest

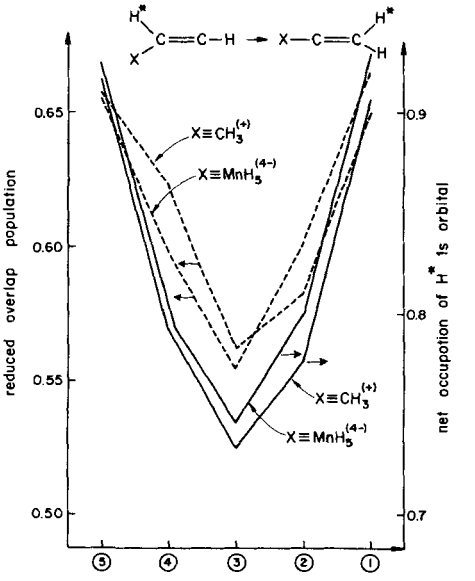

Fig. 12. *Reduced overlap population between H* and the main frame* (dashed line) *and net occupation of H* is* (solid line) *for the isomerizations* **23**→**15** *and* **21**→**19**

[12]) At this point, the reliability of the hydride model was checked by plotting the same data for ML_n = Mn(Cp)$(CO)_2$. The curves obtained are virtually identical to those featuring the hydride model.

of the molecule along the reaction path for both systems. The occupation of the 1s orbital is also plotted. At all stages of the shift substantial electron density is retained on the hydrogen. *Fig. 12* shows that at the transition state the 1s orbital is filled by 0.73 electrons. The reduced overlap population curve clearly establishes that the H atom is consistently well-bound to the remaining portion of the molecule. An interaction of type **31** is operative; at the transition state the 1s orbital forms a bonding combination with the in-plane π component.

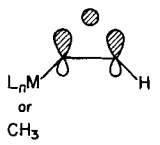

31

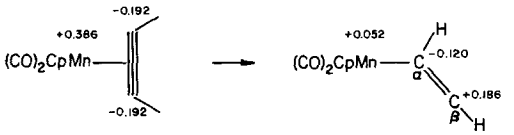

32

Let us now summarize the results we have obtained so far and their chemical implications. First, a fully concerted mechanism is not likely to be operative for the H shift. A prior slippage from η^2 to η^1 of the alkyne appears to be mandatory. This change of hapticity in an alkyne complex has been suggested several times in the past [27][13]). What has not been settled yet is the charge polarization in the ensuing η^1 complex. This certainly depends highly on the metal, its formal oxidation state, and the ligands surrounding it, as pointed out by *Otsuka* and *Nakamura* [28]. Our calculations for the realistic molecule show the changes in electron density indicated in **32**. The metal is partially reduced in the process whereas C_β becomes positively charged. Perhaps we find here the reason why the presence of basic alumina was shown [1a] to enhance the H shift in the particular case of $MnCp(CO)_2$. The presence of donor groups near C_β should stabilize the η^1-geometry.

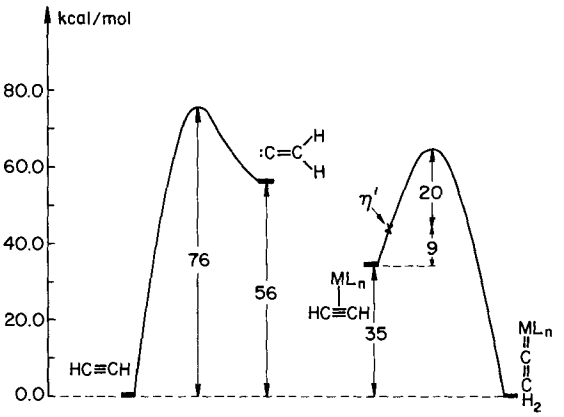

33 **34**

[13]) The intramolecular formation of a vinyl complex from a η^2-alkyne bound to a metal alkyl may also feature such an initial slippage to η^1 [27i].

This off-center slippage of the ML_n is reminiscent of what was predicted in an earlier study of nucleophilic attack on η^2-olefin complexes [29]. In the present case, we believe it serves as the starting point for the H shift. This is certainly highlighted by the organic analogy, using mode 2 (**27b**) for the fragmentation.

From the standpoint of the acetylene-vinylidene rearrangement does the ML_n piece *catalyze* the isomerization? The ambiguity that arises here is due to the switch in thermodynamic stability between the acetylene and the vinylidene upon coordination to a metal center; this is summarized in **33** and **34**. As discussed earlier, it costs 20 kcal/mol to convert the η^1 geometry into the vinylidene complex. The former lies 9 kcal/mol above **14**. A barrier of 29 kcal/mol is therefore associated with the overall process. These are all computed, not experimental, numbers. If the η^1 complex lies in a shallow minimum, the total activation energy is even less than this.

Another way to indicate the role of the metal is to take the total energy of $(C_2H_2)ML_n$ along the computed energy path for the rearrangement, and to subtract from it the energy of the ML_n fragment. What remains behind is the sum of the energy of C_2H_2 and the stabilization that fragment gains on complexation to the ML_n moiety. The resultant curve can be plotted on the same scale as the energy of isolated C_2H_2 undergoing the same rearrangement. This is shown in **35**.

Note the clear picture that results. The stabilization of the C_2H_2 fragment is much greater on the vinylidene side. This stabilization 'reaches back' into the transition state region to produce a lower activation energy for the overall reaction.

35

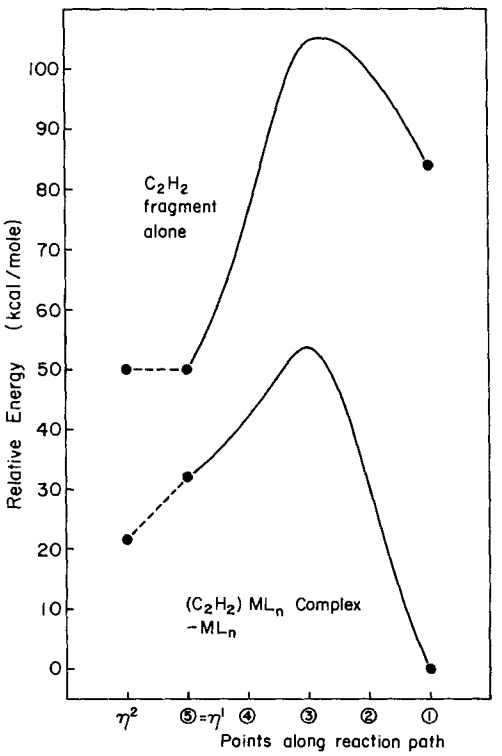

Let us examine the factors which may influence the magnitude of the barrier for the **14**-to-**15** rearrangement. Referring to *Fig. 9*, the lower a_1 is, the better it will stabilize π_i. The former is σ antibonding with respect to the ligands. Electronegative weak σ donors should push a_1 down. One must, however, be aware of the induced stabilization of the initial acetylene complex that will also result. Fragment molecular orbital a_1 is indeed much involved in the bonding between ML_n and the acetylene at the η^2 geometry. This may be seen in *Fig. 4*, where its label is 3a'. The exact role of a_1 (3a') in stabilizing both the transition state and the reactant is ambiguous, defined by a delicate balance. This is not true for 2a', *Fig. 4*, or alternatively d_{yz} *in Fig. 9*. This orbital can destabilize the acetylene complex without much of an influence on the transition state. There is much less mixing between d_{yz} and π_o than between 2a' and π_p in the η^2-alkyne complex. The reason behind this is the overlap difference: $< 2a'|\pi_p > = 0.129$ *vs.* $< d_{yz}|\pi_o > = 0.083$. Ligands with enhanced π-acceptor ability should send this metal d-centered orbital down in energy[14]).

Before moving to the next section dealing with an alternative pathway for the isomerization of C_2H_2 into CCH_2 upon complexation to an ML_n unit, we would like to explore some further ramification of the isolobal analogy. We have carried out above the isolobal substitution of the ML_n unit by CH_3^+ or H^+. One may wonder about the possibility of the reverse replacement which substitutes the *migrating* hydrogen by an isolobal $M'L_n$ fragment such as $AuPR_3$, $MnCp(CO)_2^-$ or SnR_3. The reaction is now **36**. Amusingly, if $M'L_n$ is $MnCp(CO)_2^-$, the ground-state **36a** and the transition state **36c** are degenerate, as shown in another way in **37**. The $MnCp(CO)_2$ fragment formally receiving the negative charge is

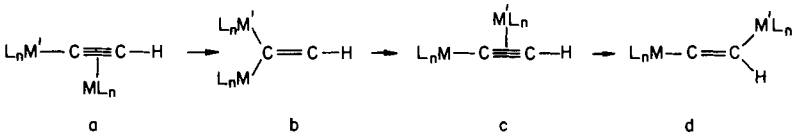

36

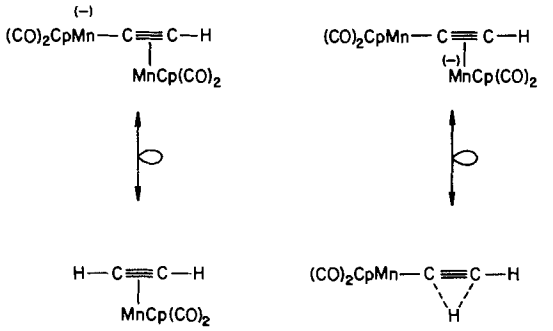

37

[14]) If the transition metal fragment does catalyze the isomerization, the geometry of the hydrocarbon fragment at the transition state ③ should be distorted towards that of the vinylidene more than in the free ligand case. The surface *in Fig. 6* is, *helas*, not accurate enough to provide us with this information.

38

electronically equivalent to a H atom. Finally, if sequence **36** represents the mechanism for the isomerization, one would expect that if M and M′ are tied together by a M–M interaction **36a** and **36c** should easily interconvert without proceeding to **36d.** Such a σ–π isomerization of a binuclear acetylide complex has been recently reported [30] and is shown in **38.**

An Alternative Pathway: Oxidative Addition Followed by Migration of H* to the Far C Atom. – In the process of building up **21** and **23**, we mention briefly the possibility of some attractive interaction between the metal and H*. This leads us naturally to examine an alternative way to produce the vinylidene complex, according to the following sequence: The first step has been dealt with previously. It is an easy deformation. **23** to **39** is an oxidative addition across the C–H bond. Finally, the hydrido-acetylide complex **39** undergoes migration of H* to C_β to produce **15.**

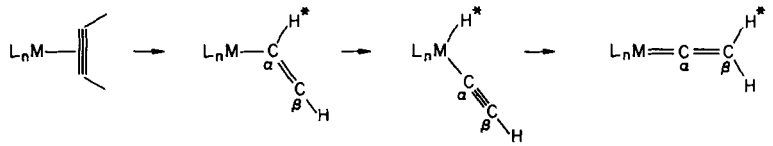

14 **23** **39** **15**

We examined in some detail both steps of this hypothetical mechanism, using MnH_5^{4-} as a model for ML_n. Central to these steps is the hydrido-acetylide **39**, a seven-coordinate complex. We assume a capped trigonal prismatic geometry, **40**, for it. The angle θ was set at 70.0° and the H atoms initially in the xy plane relaxed in the $-z$ direction by an angle of 10.0°. The bonding in seven-coordinate complexes has been the subject of a previous study [31]. Here, the molecular orbitals of **39** may be derived[15]) from those of a bent six-coordinate $d^6H_5Mn{-}C{\equiv}CH^{5-}$ *unit interacting with an empty s orbital.* The bent complex **41b** can in turn be derived from an octahedral complex **41a.**

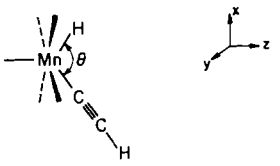

40

[15]) For a nice illustration of this formal approach in dinuclear organometallic chemistry see [32]. The formation of $(PR_3)_2HPt$-$Mo(Cp)(CO)_3$ is reported from $(PR_3)_2HPtCl$ and $NaMo(Cp)(CO)_3$. This may be viewed as the electrophilic attack of d^8–$(PR_3)HPt^+$ on d^6–$Mo(Cp)(CO)_3^-$.

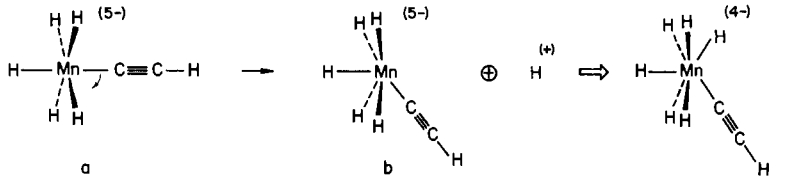

a b 41 42

The distortion **41a**→**41b** allows mixing between the symmetric component of the e_g set and one component of the t_{2g} set. This mixing follows the usual rules of perturbation theory: the lower orbital destabilizes the upper one and *vice versa*. This is shown schematically in **43**.

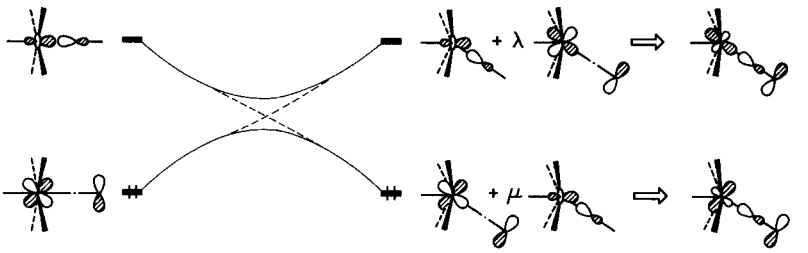

43

Note that the lower, filled orbital is beautifully hybridized toward the vacant site. It forms a nice σ bond with a proton coming in along the seventh coordination direction. A simplified version of the interaction diagram is given in **44**. A left is the pseudo-t_{2g} set filled in **41b**. Next are the two π components π_i and π_o. There is some metal-d character in these two, but only to a small extent. Finally, below this pair lies the σ bond between the metal

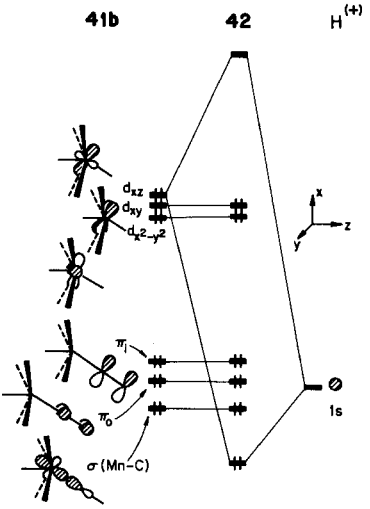

44

and C_α of the acetylide. Starting with a formally empty s orbital, its net occupation after interaction is 1.29 electrons. This is understandable in view of the excellent overlap existing between 1s and d_{xz}, $\langle 1s|d_{xz}\rangle = 0.28$. Note the oxidation of the metal atom in the process. This is what would be expected formally, as one moves from the d^6 six-coordinate complex to a situation where only two out of the three d orbitals are left non-bonding, *i.e.* a d^4 system. This is the common electron filling for seven-coordinate complexes [31]. The hydrido-acetylide complex **42** is computed to lie at the same energy as the η^1-alkyne.

Let us now turn to the oxidative addition reaction *per se*. An idealized one-dimensional path was computed taking the η^1-alkyne complex into the hydrido-acetylide **42**. A reasonable barrier of 29 kcal/mol is associated with this reaction, which is a symmetry-allowed one.

The overall process which produces a hydrido-acetylide from an η^2-alkyne costs 38 kcal/mol in our calculations. It is likely to be less than this in reality, given the geometrical and computational approximations used in this work. This reaction is believed to occur as the initial step in the alkyne oligomerization sequence [28] [33] [34]. Strong experimental evidence for the oxidative addition of a transition metal fragment across a C–H bond with an η^2-alkyne as a starting point has also become available lately [35]. Our calculations point to the normal nature of such an oxidative addition.

We move now to the H migration from the metal to C_β of the acetylide, yielding the vinylidene complex. One realizes rapidly that a bending of the acetylide at C_α is necessary, if this migration is to occur. A full potential energy surface describing the shift would involve the variation of many variables, hence, some simplifying assumptions must be made[16]). We analyzed the reaction in two conceptual stages, outlined in **45**: first, the Mn–C_α–C_β frame was bent; second, H* was shifted over to C_β, with concomitant unfolding of the frame to restore a linear Mn–C_α–C_β axis. The obvious difficulty which

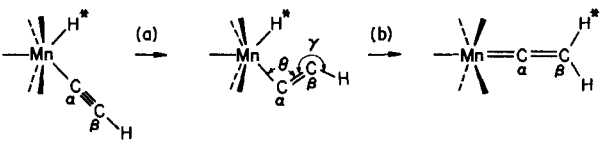

45

arises is that the two steps are not independent. In other words, the system must find a compromise between the energy cost induced by bending the acetylide and that involved in the breaking of the M–H bond.

What are the electronic consequences of varying θ without moving H*? The potential energy surface for such a distortion is shown in **46**. The superimposed dashed curve describes the distance between C_β and H*, plotted with respect to the right-hand vertical axis. The computed activation energy is high. The energy drops around $\theta = 90°$ because of the proximity of H* to C_β. The angle γ (see **45**), independently varied with θ, optimizes for $\theta = 90°$, well over 180°. This certainly creates a vacancy at C_β and makes some room

[16]) An excellent discussion of the problems associated with the computation of potential energy surface is found in [36a]. See also [36b].

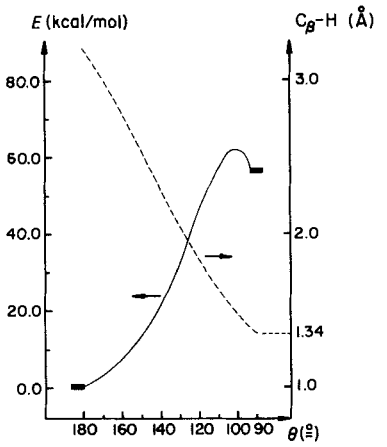

46

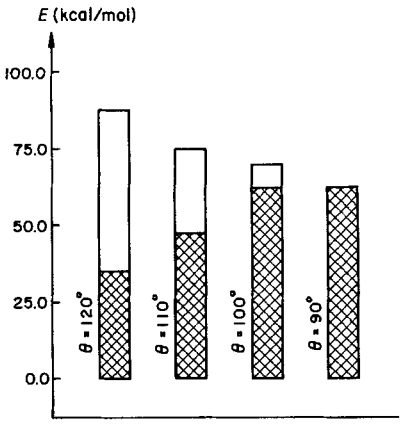

47

for H*. If one looks at the charges on each atom for step (*a*), one sees drastic changes from $\theta = 120°$. There is an accumulation of electron density at C_α. The in-plane π orbital destroyed in the distortion tends to localize the corresponding electron density on this site to produce a lone pair housed in an sp^2-type of hybrid. Conversely, a positive charge builds up at C_β. The hydride will ultimately fill in this vacant orbital. We will return to this shortly.

In a search for a compromise reaction path adopted by the system for sequence **45**, H* was migrated from the metal to C_β with the remaining part of the molecule frozen, at $\theta = 120°, 110°, 100°$, and 90°, and γ appropriately adjusted. The resulting picture for the energy is presented in the bar diagram **47**. At the bottom of each bar, the geometry is that of the hydrido-acetylide complex. The cross-hatched areas correspond to the energy required to bend the acetylide up to the particular values of θ indicated. The white areas measure the amount of energy involved in the migration of H* from Mn to C_β. Note that the bottom areas for $\theta = 100°$ and $\theta = 90°$ are identical. The activation energy for bending is indeed the same, see **46**. Also, there is no barrier to shift the hydrogen for $\theta = 90°$. Referring back to **46**, the distance between C_β and H* is only 1.34 Å at this value of θ. No wonder that the completion of the transfer is free of activation energy.

If for the time being the high numerical values of the activation energy are disregarded, diagram **47** tells us that it is easier for the system to undergo the bending distortion than to break the M–H bond.

To obtain an overall view of the entire sequence, an idealized path was computed, still within the framework of the two steps (*a*) and (*b*) introduced in **45**. The acetylide is bent up to 90° first, and subsequent migration of H* and simultaneous unfolding of the skeleton take place to reach the final vinylidene geometry. The associated *Walsh* diagram is displayed in *Fig. 13*. The orbitals at both the extreme geometries need no further comment. We have encountered them earlier in the text. In the initial stages of the reaction, the LUMO is strongly pushed down in energy by the C–C in-plane π^* orbital. The result is an orbital bonding between C_β and H* at the end of step (*a*). The metal-d orbitals rise slightly in energy. For d_{yz}, the explanation for this rise resides in the shortening of the metal to C_β distance upon bending. We find the most dramatic changes in the

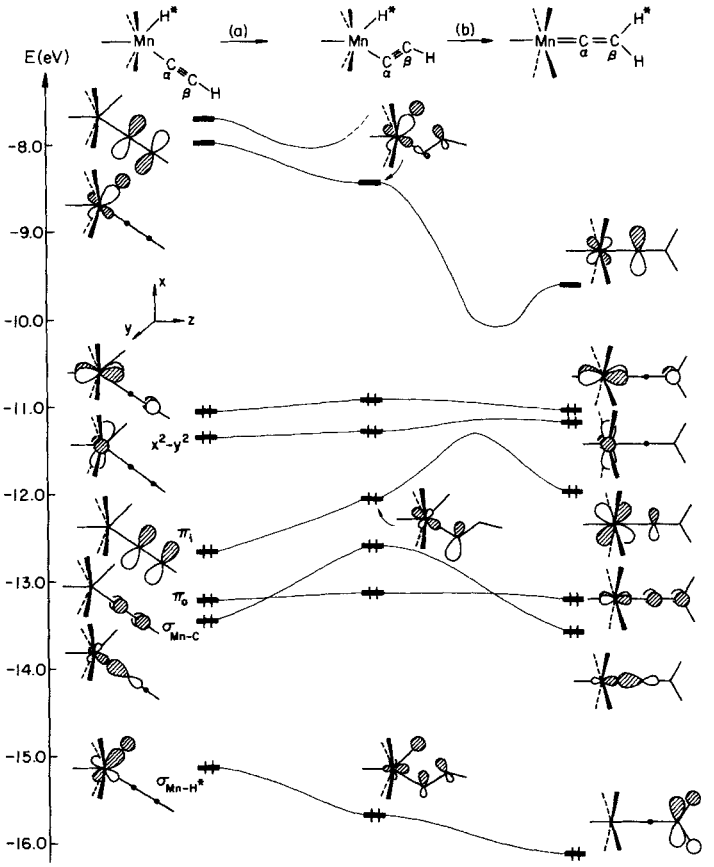

Fig. 13. *A* Walsh *diagram for the H shift from Mn to* C_β *in* **45** (see text)

lower orbitals. The in-plane π bond is broken and the corresponding orbital, π_i rises steeply in the process. At the transition state, (end of step (*a*)), it emerges as the lone pair on C_α. Please recall our earlier comment on the charge distribution at this geometry. Further down, the M–H* and M–C_α bond orbitals mix; the upper one, σ(Mn–C), is consequently destabilized whereas σ(Mn–H*) is pushed down. The latter may be viewed as a 2-electron-4-center bond at the transition state, due to the in-phase relationship

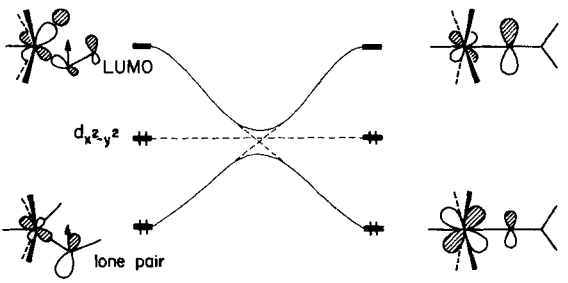

extending over the 4 centers. In step (*b*), a strong M–C_α σ bond is retrieved and the corresponding MO is much stabilized. Similarly, completion of the H transfer sends the lowest MO deeper in energy. The most interesting feature of this part of the diagram is the avoided crossing between the LUMO and the orbital sheltering the C_α lone pair. This is perhaps better shown in **48**. The LUMO goes down because of the previously noted bonding interaction between C_β and H*. It is technically prevented from going further down by non-bonding d_{x2-y2}. In practice, the crossing involves the next symmetric orbital, *i.e.* the lone pair. To put it in another way, the metal-d-centered orbital serves as a buffer between the LUMO and the C_α lone pair. For the same reason, this orbital does not rise much in energy.

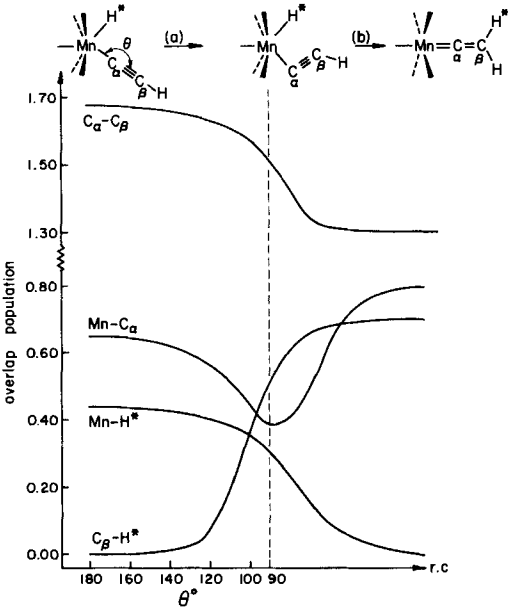

Fig. 14. *Selected overlap populations for an idealized one-dimensional rearrangement* **45** (see text)

The consistency of the reaction path chosen was checked *via* a plot of the overlap population changes occurring in the broken and formed bonds. The resulting curves are displayed in *Fig. 14*. The vertical dashed line separates the two steps (*a*) and (*b*). The absence of discontinuity in the curves at their intersection with this line is again encouraging. As could have been anticipated, the C_α–C_β overlap population drops. With a fixed Mn–C_α bond length, the overlap population reflects nicely the weakening of this bond in the beginning, then its strengthening at the vinylidene geometry. Notice that the action in terms of H* really starts at $\theta = 120°$. The Mn–H* bond weakens and H* begins to feel the presence of C_β. Along the bending motion only, the steady weakening of Mn–H* is reflected by the behavior of the lowest MO in *Fig. 13*. At the end of the first step, this level is somewhat delocalized over 4 centers, at the expense of the initially pure Mn–H* bond. The C_β–H* curve can be analyzed along the same lines.

Returning to the numerical values for the energy, the transition state is computed to lie $\sim$ 3.0 eV above the hydrido-acetylide complex. We have good reason to believe that

this energy is overestimated. For example, extended *Hückel* calculations tend to overestimate the strength of a M–H bond. This means that the angle θ must close all the more, to counterbalance the energy required to strip the hydrogen off the metal. Nevertheless we still believe in a pretty high activation energy for the process. Looking back at the *Walsh* diagram, one sees that the main source of trouble is the C_α lone pair orbital, which rises steeply in energy along the reaction path. A small cation such as Li^+ or Na^+ might stabilize this orbital and mitigate its increase in energy. Notice also the constant drop of the LUMO in *Fig. 13*. This suggests that reduction of the (certainly long lived) hydrido-acetylide complex would produce the vinylidene compound with essentially no activation. That might be a feasible process under electrochemical conditions.

To our knowledge, there is no experimental evidence concerning the conversion of an alkyl-acetylide into a vinylidene complex. This is consistent with the high energy of activation discussed above. There is one case where the hydride reaction has been observed [37] **49a**→**49b**. This is in fact a rather slow process.

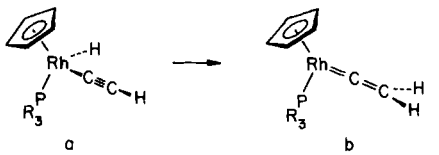

49

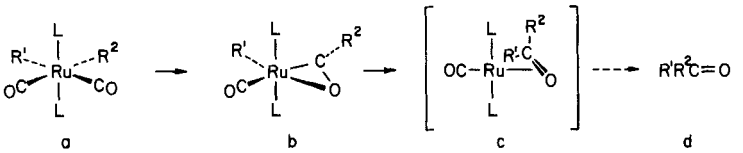

50

Let us digress here to discuss briefly a type of reaction which can be regarded as a disguised version of the hydrido-acetylide-to-vinylidene rearrangement. Take for example the recently reported [38] sequence shown in **50**. The first step is a carbonyl insertion into a M–R bond. A theoretical analysis of this process is available elsewhere [39]. Although in the original paper **50b** was not written in an η^2-acyl formulation, we believe that it might be such; an η^2-acyl formulation would put Ru in a satisfactory 18-electron configuration, and η^2-acyl complexes are now well established [40a–e]. In particular, the analogue of **50b** (R^2 just substituted by I) has been the subject of an X-ray structure determination [40d] and shown to be η^2. The bracketed complex was not detected in this sequence but strong spectroscopic evidence for the existence of such a species was found by *Schrock* and coworkers in an analogous reaction [40f]. The reverse reaction **50b**→**50c**, taking an η^2 formaldehyde into an alkyl-η^1-acyl complex, was incidentally also reported [41].

Now, take the hydrido-acetylide complex and suppose C_β undergoes oxidative addition to the metal as indicated in **51** (irrelevant ligands have been omitted). The C_2H piece behaves as a four-electron trianionic fragment. Specifically, C_α can be thought of as

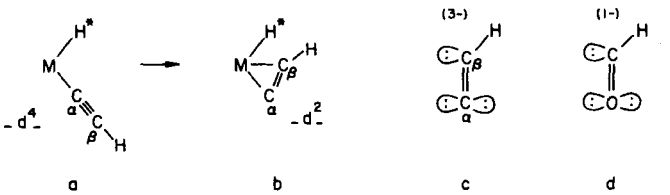

51

bearing two lone pairs. One is donated to the metal to form the σ-bond, the other one is that formed when the acetylide is bent. This fragment then looks like **51c**, isoelectronic with an acyl unit **51d**. And **51b** appears analogous to an η^2-acyl unit bound to a metal hydride fragment. Returning to **50**, the formation of the ketone amounts, *via* this analogy, to the reductive elimination **52**. Of course, the analogue of the vinylidene complex is not likely to be observed since it features an η^1-O-bound ketone. The formation of a ketone from dialkyl transition metal complexes in the presence of CO is well-documented [27h] [42]. The sequence shown in **50** is the likely route for these reactions.

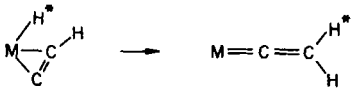

52

This analogy with acyl chemistry makes the hydrido-acetylide sequence for the acetylene→vinylidene rearrangement quite attractive. However, one must realize that the analogue of C_β in the acetylide complex is bound to the metal to begin with in the acyl complex. This overcomes the costly step energywise in the hydrido-acetylide case, which is the distortion of the $M-C_\alpha-C_\beta$ skeleton. Also, within the framework of the metal chosen in this study, (ML_5 fragment), computations show quite a bit of steric interaction, since if **51b** were to form the metal would be eight-coordinated at this point.

In this section, we have gained an understanding of the possible intramolecular reaction of an η^2-alkyne complex leading to a vinylidene complex[17]). The formal 1,2 H shift must involve the prior slippage of the alkyne to a η^1 mode of coordination. From there the vinylidene complex may be formed. The tremendous thermodynamic stability of the product and an efficient stabilization of the transition state by the metal combine to make this reaction feasible. Alternatively, oxidative addition may occur to form an hydrido-acetylide complex. Our feeling is that the hydrido-acetylide channel is a dead end, as far as eventual vinylidene production is concerned. We think the expenditure of energy to promote the migration from the metal to C_β of the acetylide is prohibitive.

Hydrogen Shifts in Binuclear Complexes. – We examine here the possibility of a rearrangement which isomerizes a binuclear acetylene complex into a vinylidene complex. Binuclear acetylene complexes may be partitioned into those possessing a parallel orientation and those with the C–C axis perpendicular to the M–M axis, the perpendicular ones.

[17]) The reverse reaction taking a vinylidene complex into an η^2-alkyne was suggested to occur in [43].

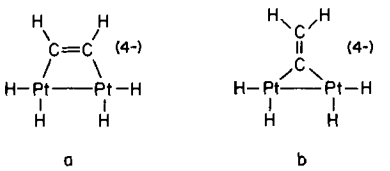

53

A molecular orbital picture for these two classes of complexes has been given in [44]. It was, in particular, asserted that in the perpendicular geometry the acetylene behaves as a neutral 4-e$^-$ donor whereas a parallel acetylene contributes 2 electrons to the system. In a vinylidene complex, the C_2H_2 unit behaves like a carbene and provides 2 electrons to the organometallic fragment. To maintain the electron count the same, this suggests that a parallel binuclear complex might be a better candidate for an isomerization to a vinylidene geometry. With this idea in mind, we look at a simple model system **53a**. Our conclusions are easily extended to different, but isolobal fragments. Again the choice of hydrides as metal ligands was dictated by computational economy. The geometry of the Pt_2H_4 unit was taken from the X-ray results of ($CO_2MeC{\equiv}CCO_2Me$) $Pt(PR_3)_2(CO)_2$ [45]. The corresponding vinylidene complex **53b** is computed to lie 5.0 kcal/mol above **53a**. The electronic structure of **53b** is reasonable, and as we noted before [44b] this complex should be synthetically accessible.

54 **55** **56**

If one begins the isomerization from **53a**, one has to break a C–H and a Pt–C bond to reach the transition state leading to **53b**. Just as in the mononuclear case, the Pt–C bond is more fragile. Small computational variations of θ and ϕ (defined in **54**) show this. A reasonable transition state geometry is depicted in **55**. The Pt–C_β bound has been broken whereas H* is still bound to C_α. The disappointing result is the energy of such a structure: ~ 3.0 eV above the acetylene complex. The reason for the high energy is easy to trace. At this point, the HOMO becomes essentially an orbital which is M–M antibonding, **56a**. In the reactant, this orbital is nicely stabilized by the LUMO of the acetylene, as shown in **56b**. This interaction is totally lost in **55**. The subsequent breaking of the C–H bond in **55** adds another 1.5 eV to the barrier. Elongation of the Pt–Pt bond certainly improves these values, but only to a limited extent. Despite numerous test calculations in quest of a reasonably low transition state geometry, our efforts were not successful. The conclusion has to be faced: the isomerization of **53a** into **53b** is not a likely process. In fact, among the dozens of binuclear acetylene complexes synthesized to date, none, to the best of our knowledge, has ever been reported to undergo the transformation into a vinylidene. As mentioned in the introduction, dihaloacetylenes produce vinylidene complexes, but intermediate acetylene complexes were not detected [5]. Binuclear vinylidene complexes obtained from alkynes have been reported; they, however, are generated by initial formation of *mono*nuclear vinylidene complexes which react further with organometallic fragments present in the reaction mixture [2a, e] [46].

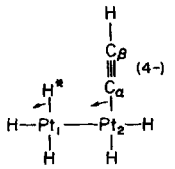

57

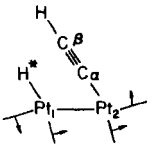

58

Is there another way one could *intramolecularly* form a binuclear vinylidene complex such as **53b**? Let us take the hypothetical hydridoacetylide **57** as a possible starting point. A potential energy surface moving H* to C_β and C_α to Pt_1 exhibits an enormous energy hill, ~ 5.0 eV. The reason for this lies in the repulsion between H* and C_α, or more specifically, between H* and the coplanar π system of the acetylide. This suggests that one might move H* *away* from the acetylide as the Pt_2–C_α bond is forming. The distortion shown in **57** with arrows achieves this. Geometrical readjustment of the two pairs of ligands on Pt_1 and Pt_2 leads to **58**, lying 1.0 eV above **57**, with limited geometry optimizations. In the motion to **58**, we have taken H* out of the way of the π system and moved C_α closer to Pt_1. We compute a further activation energy of 2.0 eV for the subsequent isomerization of **58** into the binuclear vinylidene **53b**. A complementary perspective on this reaction is obtained by realizing that the transformation of **57** into **53b** is an internal reductive elimination occurring on a binuclear framework. This reaction type was analyzed recently by one of us [47] and found to be symmetry-forbidden for a least-motion pathway. What we have at hand in **57**→**53b** is a weak avoided crossing and a lower activation energy occasioned by the much lower symmetry path. In *Fig. 15* are shown the changes in overlap population and net charges during the course of the transit from **57** to **53b**. All the bond transformations are clearly displayed. Although the path seems relatively smooth, one should notice that the breaking and formation of the Pt–H* and C_β–H* bonds are not quite simultaneous. In the early stages of the reaction, the Pt_1–H* bond is dismantled without any effect on the C_β–H* bond. The two curves cross at a

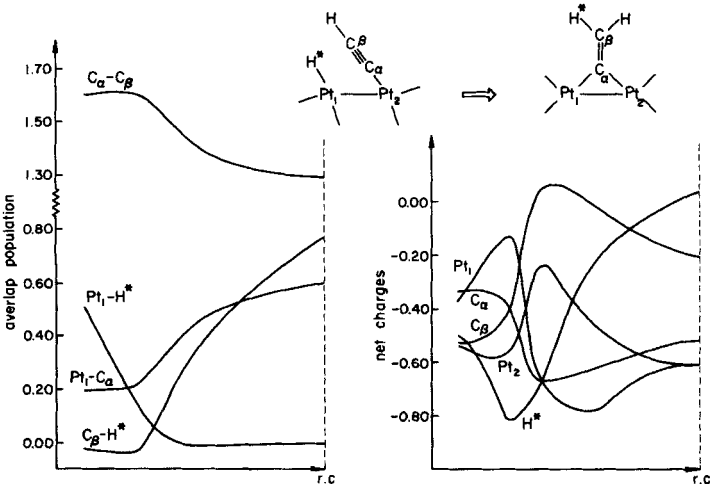

Fig. 15. *Selected overlap populations* (left) *and net charges* (right) *going from* **58** *to* **53b**

rather small value for the overlap population. This simply means that our path, if computationally convenient, is not quite the best one. Note, however, the nice decrease in the C_α–C_β bond strength. Let us turn to the charges. Apparently, the Pt_1–H* electron pair goes to the hydrogen. The charge on Pt_1 increases, whereas the reverse is true for H*. Now look at C_α and C_β. The former sees an accumulation of electron density and the latter a build-up of positive charge. At the transition state, the polarization is that of **59**. This is an important piece of information in regard to possible substituent effects. We return to this subject shortly.

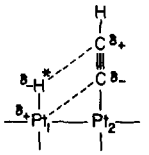

59

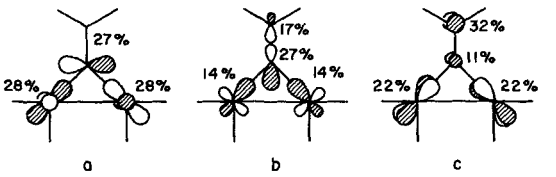

60

The reader at this point may be puzzled by the charge distribution in the vinylidene complex in *Fig. 15*. C_α is more negatively charged than C_β. The reason for this lies in the presence in **53b** (as well as the carbonyl-substituted analogue) of two filled molecular orbitals relatively localized on C_α: these are **60a** and **60b**. They descend from the vinylidene fragment LUMO and HOMO, respectively. The attack of, say, a proton along the direction of the electron density of C_α is obviously unfavorable in both **60a** and **60b**. The proton would have to approach C_α in the molecular plane. Also, substantial geometrical changes would have to take place in order for C_α to attain reasonable hybridization. Our proton must have another choice. It actually has, *via* molecular orbital **60c**. The latter is primarily concentrated on C_β and the metal atoms, but more importantly, the lobes on C_β point perpendicular to the molecular plane. Also one should realize that only a small geometrical distortion can accomodate an eventual sp^3 hybridization at C_β after completion of the proton addition along this direction. The idea emerges that electrophilic addition on the binuclear vinylidene complex **53b** is frontier-orbital-controlled and not

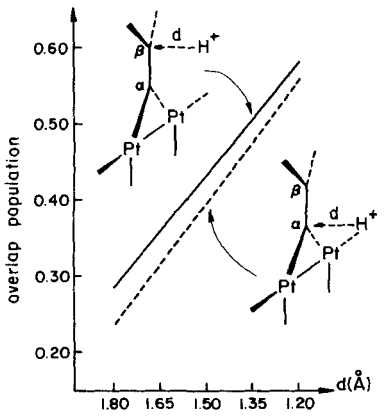

61

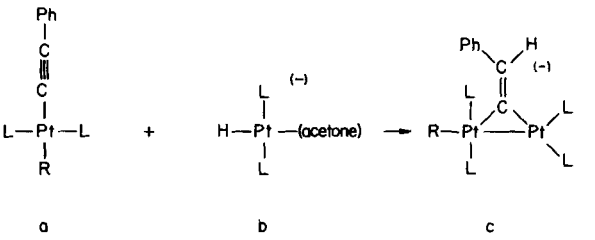

62

charge-controlled. In other words, the topological difference between potential donor orbitals favors an attack at C_β and wins over simple electrostatics which would indicate to an addition at C_α. These predictions were numerically tested by approaching a proton to C_α and C_β along the two directions defined in **61**. The calculation was done with CO's at each Pt. The solid curve represents the overlap population between C_β and H^+ at various distances, d, whereas the dashed line refers to the overlap population between C_α and H^+. Clearly a stronger interaction exists when the H^+ attacks at C_β. A plot of the energy (not shown here) along these two paths further shows that the channel for addition to C_β is of lower energy, 5.5 kcal/mol in average, than that for an attack on C_α.

The reaction which takes the hydrido-acetylide into a binuclear vinylidene may be regarded as a [2 + 2] addition, a process believed to be common in catalytic reactions [48]. Alternatively, it represents the insertion of a C≡C bond into a M–H bond. The feasibility of such a reaction finds some experimental support in mononuclear organometallic chemistry [49][18]). The generation of a binuclear vinylidene complex *via* the route outlined above has, however, never been observed. However, something close to it has. Take the recently reported [50a] reaction shown in the sequence **62a–c**. A mononuclear acetylide adds to a Pt hydride complex. The mechanism suggested involves **63** as the intermediate, which then undergoes 1,2 addition of the M–H bond across the acetylide triple bond, with concomitant formation of the M–M bond. The latter arises from formal donation of an electron pair of d^{10}-Pt_1 into d^8-Pt_2. Another view of **63** is offered in **64**, which emphasizes better its resemblance to **58**. The difference lies only in the character of the M–M bond. In **58**, the two metal atoms are d^9 and a pure covalent bond is formed, as opposed to **64**.

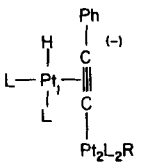

63

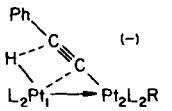

64

Backtracking a little, one can see in *Fig. 15* that *initially* C_β is more prone to attack by an electrophile than C_α. This agrees with experimental observations [24]. However, the polarization of the Pt_1–H* bond favors a negative hydrogen, which appears to contradict previous suggestions [50b]. Calculations with more realistic CO ligands afford the same conclusion.

A detailed examination of the *Walsh* diagram for the transformation **57**→**53b** shows that mixing of the LUMO and HOMO of the reactant is important along the reaction path. The activation barrier should be reduced by lowering the LUMO, which is Pt_1–H*-σ-antibonding but also σ-antibonding with respect to the other two ligands. Weak σ donors at Pt_1 should put this orbital at relatively low energy. The charge distribution changes, as indicated schematically in **65**. It is obvious that electron density is required at C_α to promote the polarization **65b**. In other words, we aim at making the acetylide a poorer σ donor. This may be achieved by a strong σ-donor substituent *trans* to C_α on Pt_2.

[18]) For insertion of alkyne into metal alkyl, see [49c].

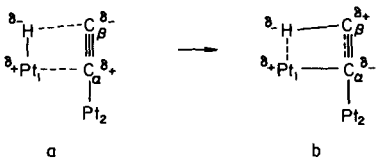

65

All in all the formation of a vinylidene complex from a hydrido-acetylide binuclear complex appears to be a feasible process. We eagerly await the report of such a transformation in the ever growing organometallic literature.

We would like to conclude this section on H shifts in binuclear complexes by examining reaction (*2*) (see early part of the text) in some detail. It involves the isomerization of a μ-vinyl di-iron complex into a μ-alkylidyne. The information that forms the basis for the forthcoming discussion is summarized in the *Scheme*, and is taken from the work of *Casey, Marder* and coworkers [6]. The binuclear frame is a $(\mu\text{-CO})(CpFe(CO))_2$ unit, symbolically indicated by Fe–Fe. There are distinguishable steps for *rearrangement* from a bridging carbyne to a bridging vinyl group (A), and a *fluxional* process that interrelates unsymmetrical vinyl conformations (B). A further hypothetical *isomerization* process (C), by which the local configuration of R and R′ is interchanged, has so far not been observed independent of the rearrangement.

Scheme

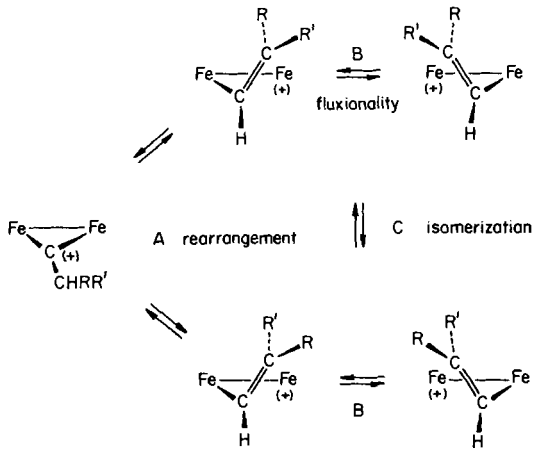

Substitution	$\Delta G^{\neq}$ rearrangement	$\Delta G^{\neq}$ fluxionality
R = R′ = H	> 32 kcal/mol	> 16 kcal/mol
R = H, R′ = $-CH_2CH_2CH_3$	27.1 kcal/mol	12.9 kcal/mol
R = R′ = $-CH_2CH_2CH_2-$	19.9 kcal/mol	10.3 kcal/mol
R = H, R′ = p-tol	—	10.3 kcal/mol

The fluxionality process in question has been investigated previously in trinuclear Os clusters [51]. Dirhenium complexes have been shown recently to undergo the same process [52]. On the triosmium cluster, *Shapley* and coworkers had demonstrated that in the transition state of (A) the CHCHR plane is perpendicular to the M–M bond bridged by the μ-vinyl group. If this carries over the di-iron complex, which we think it should, the transition state for fluxionality (A) should be represented by **66a** and not **66b**, looking down the triangle formed by the two Fe atoms and C_α. The shaded and unshaded balls stand for the two different alkyl groups on C_β. Notice, incidentally, that transition state **66b** reverses the configuration of the olefinic bond: If the shaded ball were to start *exo* to the pseudo three-membered ring, the interconversion through **66b** would put it in the *endo* position.

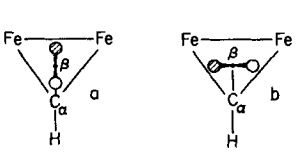

66

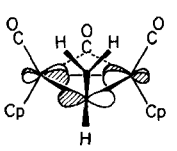

67

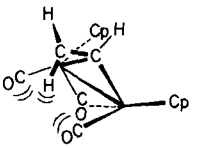

68

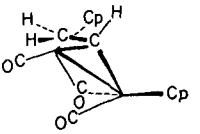

69

The alternative transition state configurations **66a** and **66b** are close in energy, but **66a** is more stable, by 4 kcal/mol. More efficient bonding between C_α and the Fe atom is attained in **66a**. However in **66b**, the HOMO, shown from a side view in **67**, contains some M–M antibonding character; this further destabilizes **66b** with respect to **66a**. Acting against this preference is a steric factor which we attempt to illustrate in **68** and **69**. In the perpendicular conformation **68** (corresponding to **66a**) one H group is close to the two CO groups as indicated. Our computations show a slight negative overlap population between this H and the two CO C atoms. This repulsion is likely to be much more important for a bulkier substituent in C_β. This leads us to think that the parallel conformation might be preferred in the case of *two* relatively bulky groups on C_β. The natural preference for **66a** might then be upset by steric problems.

But what is the transition state for rearrangement, the higher energy process A in the *Scheme*? It seems to be **66b**, not **66a**. We computed a one-dimensional surface[19]) taking the μ-alkylidyne complex into the parallel geometry **69**, as shown in **70**→**71** (ligands omitted). Note the mirror plane of symmetry maintained throughout the transformation. A reasonable barrier of 43 kcal/mol is calculated. Experimentally, the same reaction with a propyl and a hydrogen on C_β was determined by NMR spectroscopy to proceed with an

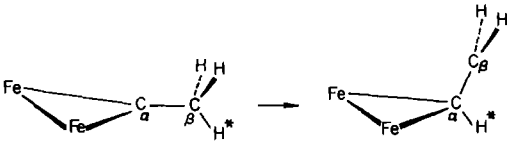

70 **71**

[19]) The calculations were performed with the CH_2 *anti* to the Cp's with respect to the Fe-Fe-C_α plane as suggested by the structure of the acylium derivative [6a].

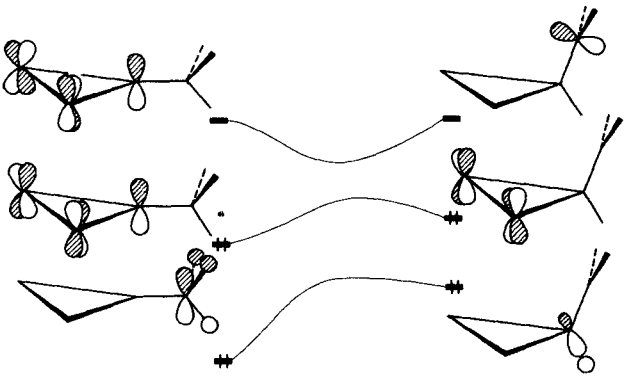

72

activation energy of 27.1 kcal/mol. It is obvious that once **71** is reached, collapse to the μ-vinyl complex occurs with no activation. The source of the barrier is two-fold, as shown schematically in **72**. The C–H* bond is broken, the corresponding orbital is boosted up. The slope of this rise is somewhat attenuated by an orbital initially π bonding between C_α and the two Fe atoms. When these two orbitals mix, the two p orbitals on C_α and C_β provide the 'bridge' for H*. More insight into the electronic changes during this process is gained from *Fig. 16*. On the left are plotted a few selected overlap populations. As correctly anticipated by *Casey* and coworkers, and confirming the picture of **72**, the transition state is characterized by a bridging position of H* between C_α and C_β. The C_α–H* and C_β–H* overlap population curves cross at a large numerical value, ~ 0.300. Notice the bond order increase for the C–C bond in the upper curve[20]).

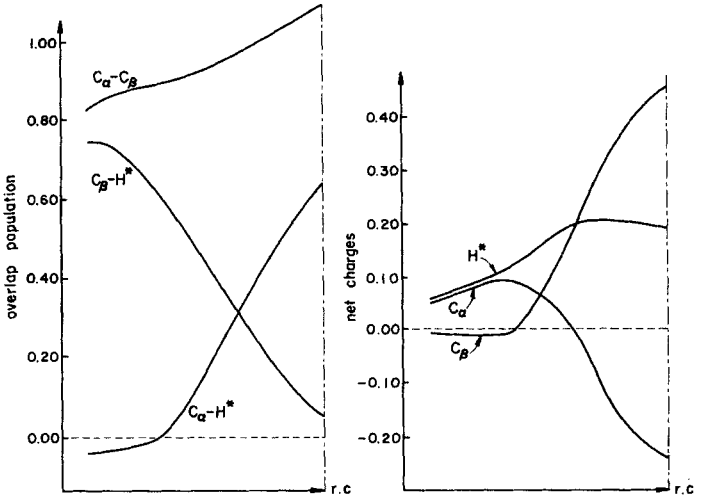

Fig. 16. *Selected overlap populations* (left) *and net charges* (right) *going from* **70** *to* **71**

[20]) The bond length was adjusted from 1.53 Å to 1.41 Å during the process.

On the right-hand side of *Fig. 16* are the net charges of H*, C_α and C_β. Initially, the bearer of the positive charge is C_α. The transfer of its cationic nature to C_β is nicely illustrated. The topology of the LUMO in **72** is also a reflection of this phenomenon.

We calculate a small activation energy, 8 kcal/mol for the reverse reaction, from the symmetric μ-vinyl structure **71**, to the μ-carbyne **70**. That this activation energy may not be zero is interesting because it opens up the possibility of observing the isomerization process C between μ-vinyl isomers differing in the configuration of R and R′ relative to H in the μ-vinyl geometry (see the *Scheme*). That isomerization would be likely to proceed through a transition state such as **71** (or **66b**). The isomerization so far has not been observed independent of the rearrangement, but perhaps there is a chance, within a narrow temperature range, of doing so.

Though we understand individually the basic stereochemistry of the fluxionality process (B) and also the stereoelectronic requirements for the rearrangement (A), we have difficulty in coming up with a merger of the two pictures. The transition state for the fluxionality should be **66a**, but it is through **66b** that H migration (rearrangement) and isomerization should take place. Yet, **66b** cannot be a true transition state, for rotation around the C–C bond, to **66a**, is in our calculations steadily downhill in energy. Complete geometry optimization might yield separate transition states for rearrangement, fluxionality and isomerization, but we suspect that one will have to go beyond transition state theory, into a trajectory formalism, to understand the branching pathways on this surface.

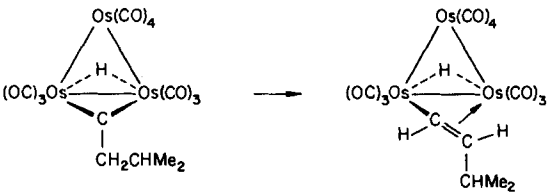

73 **74**

Interestingly, this type of H shift does not appear to be limited to cationic binuclear complexes. In fact, *Green* and coworkers recently demonstrated [53] the occurrence of such a process on a triosmium cluster, **73**→**74**. This last reaction may very well represent an example of the cluster-surface analogy pointed out in a series of articles by *Muetterties* [54]. Ethylene is known to chemisorb on Rh(111), Pt(111), and Pd(111) surfaces. Upon heating, the metal surface has been shown to be covered by a monolayer of the ethylidyne fragment $C-CH_3$ [55]. It is exciting to think that the first step in this transformation may involve a C–H scission to produce a vinyl fragment which rapidly rearranges to the ethylidyne geometry *via* the reaction discussed above.

Trinuclear Systems. – Small hydrocarbon molecules such as ethylene and acetylene have been shown recently to give rise to a wide variety of reactions when attached to a trinuclear organometallic fragment [56][21]). Cleavages of C-alkyl bonds and/or fluxionality are characteristic processes. It is our purpose in this closing section to briefly and qualitatively discuss a few of these transformations, those which entail an H shift. These are geometrically complex systems, and only limited computations were carried out.

[21]) Flipping of an acetylide on a trinuclear cluster was recently studied [56e].

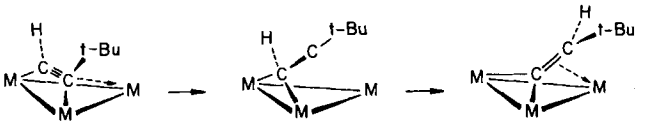

75

We begin with reaction (*3*), mentioned earlier in the *Introduction*. A remarkable feature of this transformation is its apparent simplicity. The idea of a concerted process such as **75** first comes to mind. But the energy of the would-be transition state is computed to be very high, relative to that of the starting μ-η^2-acetylene. Just as in the binuclear case, a strong bonding interaction[22]) is lost (**76**) and the two electrons left behind enter the corresponding M–M antibonding orbital.

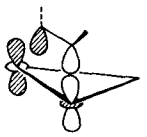

76

Based on the well-established propensity of trinuclear fragments to cleave C–H bonds [54b] [56a, c] [58], we would like to suggest an alternative mechanism, shown in **77**. Here the starting point is a conformation with the acetylene bond parallel to the Co–Co axis. A rotation by 30° produces **77b** where the acetylenic bond now bisects one Co–Ru bond. The next step is an oxidative addition of the C–H bond to form a hydrido-acetylide species. Finally, a pivoting motion of the acetylide [56e], coupled with migration of H to C_β leads to the formation of **77d**, the observed product. Let us go through each step in more detail. The initial rotation finds some experimental support in the X-ray structure of the acetylene complex. Unexpectedly, **77a** is not the geometry found. A careful look at the structure shows that the acetylenic bond is parallel to a Co–Ru bond, **78**, and that a CO has become bridging, presumably in order to readjust the electron distribution. We do not think that this surprising geometry is the result of any particular electronic require-

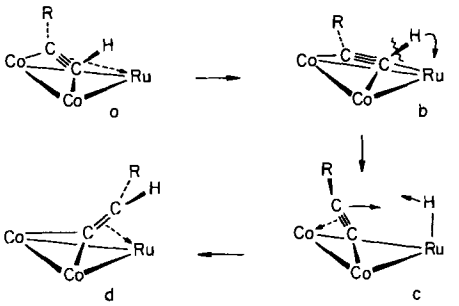

77

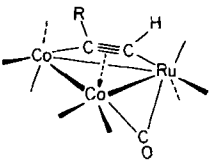

78

[22]) For a detailed description of the bonding between an acetylene and a M_3L_9 fragment, see [57].

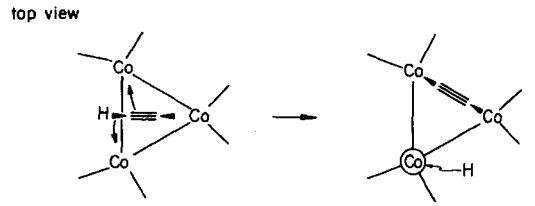

79

ment. However, it may simply emphasize a facile fluxional process in the complex. In the crystal, a particular geometry on the potential surface defining these motions is frozen. For this reason, we think **77b** is a structure attainable by the complex. The oxidative addition leading to **77c** is a less obvious process. To get an idea of the energy involved, we computed the same reaction on a model system **79** using an idealized one-dimensional transit. Starting with an acetylene in the ('wrong') perpendicular [57] geometry bound to a D_{3h} $Co_3H_9^{8-}$ cluster, the activation energy is calculated as less than 2.0 eV. The geometry of the acetylide was adapted from known structures of binuclear complexes [59]. The final location of the hydrogen is atop of the circled Co atom. Despite the gross approximation used in our procedure, we place some confidence in the magnitude of the activation energy. There are two reasons for this: the hydrido-acetylide complex formed exhibits a reasonable level pattern. Indeed, the bonding in this system is analogous to that found for a parallel bonded acetylene; two Co atoms are d^8 and attached to an alkyl group *via* a σ bond, whereas the third metal atom is involved in π bonding. Secondly, the reduced overlap population between atoms implicated in bond breaking and forming processes show a smooth variation along the path.

Finally, two factors should favor a moderate activation energy for the formation of the vinylidene complex. There is a natural tendency for the acetylide fragment to behave as a μ^3-5e$^-$ donor on a trinuclear framework [56a]. This will 'push' the C_2H unit inside the metallic triangle, hence toward the hydride. In the same vein, hydrogens are found more commonly in a bridging position rather than a terminal one in clusters, and migration of H atoms around the periphery of a multinuclear framework is well-established [56d] [60][23]). On these grounds we believe in a small barrier for moving the H-atom in the vicinity of the acetylide C_β, preceding the formation of the vinylidene.

The mechanism offered above for reaction (*3*) is obviously only one out of many possible ones. However, we feel that the truth does not lie far from it – each suggested step is in agreement with the well-documented chemistry of this type of system.

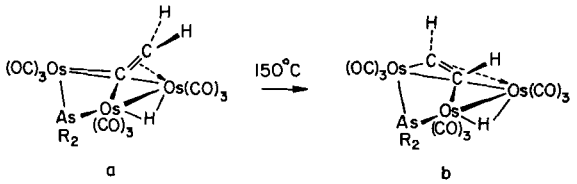

80

---

[23]) Note that H migration from a metallic frame to a hydrocarbon fragment attached to it has several precedents [53] [56a, d] [60c].

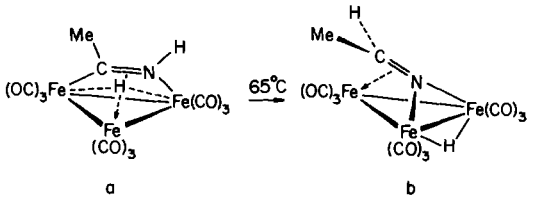

81

There are in the recent literature two reactions which involve, formally, a similar H shift. The hydrido-vinylidene complex **80a** was shown [61] to isomerize thermally to the acetylene complex **80b**. Also, a few years earlier, *Kaesz* and coworkers had reported [62] [63] the isomerization under mild thermal conditions of an acetimidoyl complex **81a** into an ethylidenimido geometry, **81b**. One may show easily the isoelectronic relationship between the systems present in **80** and **81**. Notice, however, that **81** is the reverse process of **80**. In both cases, the mechanism of these transformations was believed to involve the bridging H atom. In particular, if one deprotonates **81a** (bridging H atom), the isomerization to the anionic analogue of **81b** was found *not* to proceed. In the same study, the

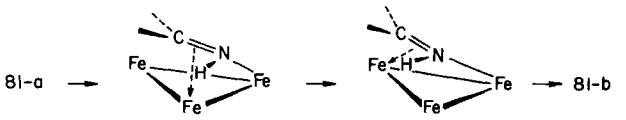

82

C-bonded H atom and the bridging H atom were demonstrated to exchange in **81b** at 35.0 °C [64][24]). On these grounds, the isomerization **81** was proposed to proceed *via* a σ–π iminyl geometry as in **82** (CO omitted). We would like to suggest another species which could be involved in this reaction, namely **83**. This idea rests on the fact that **82** represents a good geometrical starting point for the reductive elimination producing **81b**. More important is the existence in the literature of a related complex, **84**. The latter, however, possesses one more CO on the unique metal atom and the resulting absence of unsaturation has made the isolation of **84** possible [65]. The bonding in **84** was described as featuring a strongly polarized C–C bond. The CF_3 group deprives C_β of its electron density and Os acts as a weak nucleophile. The electronegativity difference between C and N certainly favors the same type of polarization in **83**. A calculation on **83** (hydrogens used instead of carbonyls) reveals a reasonable electronic structure for this species. In particular a strong bonding interaction is found between one lone pair on the N atom and

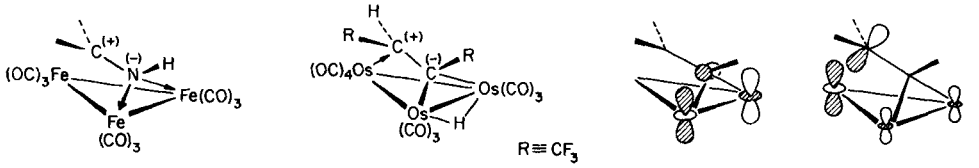

83 **84** **85** **86**

[24]) However, it was not possible to assert whether the process was intra- or intermolecular [64].

one component of the 2e set on the tri-iron fragment. It is depicted in **85**. As expected, a low-lying LUMO is the main feature of **83**. This orbital is centered on the unique iron as well as on C_β, see **86**. In **84**, the equivalent orbital is filled. Somewhat surprisingly, the energy of **83** is computed to lie close to that of **81a**. For the latter the experimentally determined [63] geometry was idealized in our calculation. We will not put excessive trust in our energy values, but **83** should be accessible to the system during the course of the reaction, although it may be hard to prove this in practice.

From **83**, an idealized one-dimensional surface was generated, leading to the final complex, **81b**. The latter lies 1.1 eV below **81a**. This oxidative addition turns out to be a relatively facile process, with an activation energy of 2.0 eV. This undoubtedly represents an upper bound to the real value. *Fig. 17* displays the change in overlap populations of interest for this process. The N–H and $Fe_{2,3}$–H curves illustrate in a nice way the chemistry going on in this transformation. Interestingly, the Fe_2–Fe_3 bond weakens upon

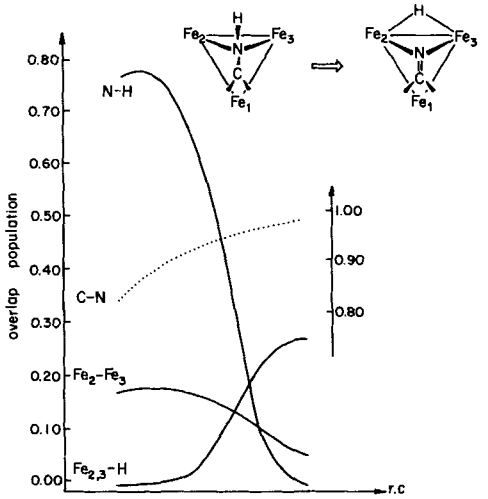

Fig. 17. *Selected overlap populations for the oxidative addition* **83** *to* **81b**. The C–N curve refers to the scale on the right-hand side of the plot.

formation of the H bridge[25]). This agrees with experimental observations [66]. The symmetric combination of the 1e set on the Fe_3 frame, initially bonding between the two Fe atoms, becomes delocalized over the third center, *i.e.* the H-atom, as pictured in **87** in a top view. Notice the sizeable increase in the strength of the C–N bond. A glance at the net charges on the H and the N atom is informative in that respect. The σ electron pair of the N–H bond ultimately ends up on the nitrogen. The hydrogen grows positive in the

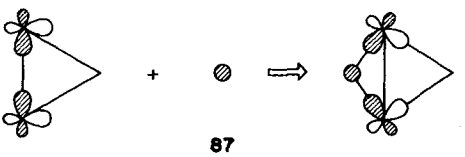

87

[25]) Again, the metallic frame was frozen in a constant geometry for this calculation.

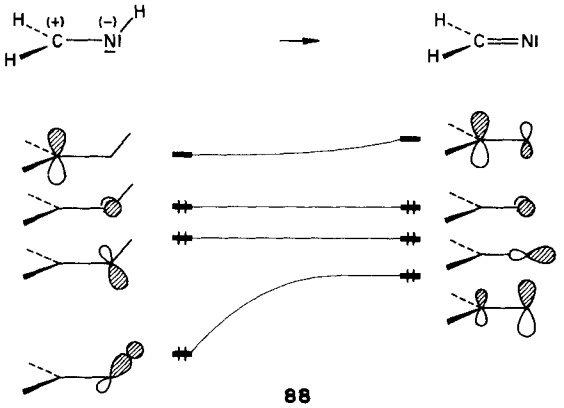

88

course of the reaction. From a localized bond-orbital standpoint, the situation is that of **88**. The N–H σ bond rises in energy (it is obviously the source of the barrier discussed earlier) and formally correlates to a π bonding orbital between C and N: the bond order increases formally from 1 to 2.

The oxidative addition examined in the previous section appears to be a likely step in reaction **81**. We believe, however, that this process is not limited to this particular sequence. Reaction **80**, or rather its microscopic reverse, is one example. In this case, there must be initial rotation of the vinylidene fragment in order for it to be in the proper orientation required by the geometry shown in **83**; vinylidenes and alkynes are known to be very mobile on trinuclear clusters [56b]. Reactions in which hydrogens transfer from the metallic frame to the hydrocarbon ligand when C_2H_4 is reacted with $Os_3(CO)_{12}$ are also likely candidates to feature such a mechanistic step [56a].

In this contribution we have tried to gain a better understanding of H migrations in hydrocarbon fragments bound to transition metal complexes. We have not explored all the reactions, particularly on binuclear and trinuclear systems, but rather we have deliberately limited ourselves to representative transformations. No doubt much more work is needed, primarily on specific catalytic reactions such as the hydrogenation of alkynes by binuclear Rh complexes [67] and on the chemistry of high nuclearity cluster with small unsaturated hydrocarbons [68][26]). From the study of the acetylene-vinylidene isomerization we find that in this kind of transformation the role of the transition metal fragment depends strongly on its nuclearity. Mononuclear units tend to catalyze effectively the reaction, whereas trinuclear frameworks might be said to just assist the process. Similarly, in the μ-alkylidyne-to-μ-vinyl isomerization, the binuclear fragment simply 'supports' the organic species undergoing the reaction. These dissimilarities in behavior may simply be a reflection of the fundamental differences existing between homogeneous and heterogeneous catalysis.

We are grateful to *Santiago Alvarez* and *Thomas A. Albright* for useful discussions, and to *C. P. Casey* and *Seth Marder* for communication of results prior to publication. Our drawings were done by *Jane Jorgensen* and *Elisabeth Fields*, and the manuscript typed by *Carol Cook*. We are grateful to the *National Science Foundation* for its continued support of this research through Grant CHE 8406119 and also by Grant DMS 7681083 to the Materials Science Center at Cornell.

[26]) Remarkable and puzzling reactions include those described in [68].

Appendix 1. – All C–H, M–H bonds were fixed at 1.10 and 1.70 Å, respectively. The C–C bond length was set at 1.32 Å when the hydrocarbon was coordinated to a metal. It was set at 1.40 Å for calculations in the free ligand isomerization. All metal–C(O), C–O distance were taken as 1.74 Å and 1.14 Å, respectively. Trinuclear frames were taken equilateral, with Co–Co = 2.46 Å and Fe–Fe = 2.65 Å. Calculations on existing complexes were run using the structural information when available.

Appendix 2. – Computations at the extended *Hückel* level were used throughout [69]. The orbital exponents, and H_{ij}'s were taken from previous work [44a] [71] [72] and are listed in the *Table*. The 'weighted' H_{ij} formula was used [70]. Parameters for H and C are standard ones [69].

Table. *Parameters Used in Extended* Hückel *Calculations*

	Orbital	H_{ii} [eV]	ζ_1	ζ_2	C_1^a	C_2^a
Co	3d	–13.18	5.55	2.10	0.5679	0.6059
	4s	–9.21	2.00			
	4p	–5.29	2.00			
Fe	3d	–12.60	5.35	2.00	0.5505	0.6260
	4s	–9.10	1.90			
	4p	–5.32	1.90			
Pt	5d	–12.59	6.013	2.696	0.6334	0.5513
	6s	–9.08	2.554			
	6p	–5.47	2.554			
Mn	3d	–11.59	5.15	1.90	0.5320	0.6490
	4s	–8.63	1.80			
	4p	–5.06	1.80			
N	2s	–26.00	1.95			
	2p	–13.40	1.95			

[a]) These are the coefficients in the double-ζ expansion.

REFERENCES

[1] a) A. N. Nesmeyanov, G. G. Aleksandrov, A. B. Antonova, K. N. Anisimov, N. E. Kolobova, Yu. T. Struchkov, *J. Organomet. Chem.* **1976,** *110,* C36; A. B. Antonova, N. E. Kolobova, P. V. Petrovsky, B. V. Lokshin, N. S. Obezyuk, *ibid.* **1977,** *137,* 55; N. E. Kolobova, A. B. Antonova, O. M. Khitrova, M. Y. Antipin, Yu. T. Struchkov, *ibid.* **1977,** *137,* 69; G. G. Aleksandrov, A. B. Antonova, N. E. Kolobova, Yu. T. Struchkov, *Koord. Khim.* **1976,** *2,* 1984; *Sov. J. Coord. Chem.* **1977,** *2,* 1300; b) M. I. Bruce, R. C. Wallis, *J. Organomet. Chem.* **1978,** *161,* C1; *Aust. J. Chem.* **1979,** *32,* 1471; c) K. R. Birdwhistell, S. J. N. Burgmayer, J. L. Templeton, *J. Am. Chem. Soc.* **1983,** *105,* 7789.

[2] a) K. Folting, J. C. Huffman, L. N. Lewis, K. G. Caulton, *Inorg. Chem.* **1979,** *18,* 3481; b) Y. N. Al-Obaidi, M. Green, N. D. White, G. E. Taylor, *J. Chem. Soc., Dalton Trans.* **1982,** 319; c) G. K. Anderson, R. J. Gross, L. Manojlovic-Muir, K. W. Muir, *ibid.* **1979,** 684; d) N. E. Kolobova, L. L. Ivanov, O. S. Zhvanko, G. G. Aleksandrov, Yu. T. Struchkov, *J. Organomet. Chem.* **1982,** *228,* 265; e) D. L. Davies, A. F. Dyke, A. Endesfelder, S. A. R. Knox, P. J. Naish, A. G. Orpen, D. Plaas, G. E. Taylor, *J. Organomet. Chem.* **1980,** *198,* C43; R. E. Colborn, D. L. Davies, A. F. Dyke, A. Endesfelder, S. A. R. Knox, A. G. Orpen, D. Plaas, *J. Chem. Soc., Dalton Trans.* **1983,** 2661; f) D. F. Marten, *J. Chem. Soc., Chem. Commun.* **1980,** 341; g) M. I. Bruce, A. G. Swincer, B. J. Thomson, R. C. Wallis, *Aust. J. Chem.* **1980,** *33,* 2605; h) A. J. L. Pombeiro, J. C. Jeffery, C. J. Pickett, R. L. Richards, *J. Organomet. Chem.* **1984,** *277,* C7.

[3] S.-B. Samuels, S. R. Berryhill, M. Rosenblum, *J. Organomet. Chem.* **1979,** *166,* C9; D. J. Bates, M. Rosenblum, S.-B. Samuels, *ibid.* **1981,** *209,* C55; H. Berke, P. Harten, G. Huttner, L. Zsolnai, *Z. Naturforsch., B* **1981,** *36,* 929; N. E. Kolobova, L. L. Ivanov, O. S. Zhvanko, *Izv. Akad. Nauk SSR, Ser. Khim.* **1980,** 478; *ibid.* **1980,** 2646; N. E. Kolobova, L. L. Ivanov, O. S. Zhvanko, *ibid.* **1983,** 956; N. E. Kolobova, L. L. Ivanov, O. S. Zhvanko, A. S. Batsanov, Yu. T. Struchkov, *J. Organomet. Chem.* **1985,** *279,* 419.

[4] M. I. Bruce, A. G. Swincer, *Adv. Organomet. Chem.* **1983,** *22,* 59.

[5] L. Papp, G. Varadi, G. Palyi, XVth (Hungarian) Colloq. Coordination Chemistry, Siofolk, May 19–21, 1980; J.T. Horvath, G. Palyi, L. Marko, G.D. Andretti, *Inorg. Chem.* **1983,** *22,* 1049; *J. Chem. Soc., Chem. Commun.* **1979,** 1054; G. Varadi, G. Palyi, *Inorg. Chim. Acta* **1976,** *20,* 233; *Magy. Kem. Foly.* **1977,** *83,* 3323.

[6] a) C.P. Casey, P.J. Fagan, W.H. Miles, S.R. Marder, *J. Mol. Catal.* **1983,** *21,* 173; b) C.P. Casey, P.J. Fagan, *J. Am. Chem. Soc.* **1982,** *104,* 4950, ref. 19; C.P. Casey, S.R. Marder, P.J. Fagan, *ibid.* **1983,** *105,* 7197.

[7] E. Roland, H. Vahrenkamp, *J. Mol. Catal.* **1983,** *21,* 233; W. Bernhardt, H. Vahrenkamp, *Angew. Chem.* **1984,** *96,* 139; *ibid. Int. Ed.* **1984,** *23,* 141; E. Roland, W. Bernhardt, H. Vahrenkamp, *Chem Ber.* **1985,** *118,* 2858.

[8] a) H.F. Schaefer III, *Acc. Chem. Res.* **1979,** *12,* 288; b) P.J. Stang, *Chem. Rev.* **1978,** *78,* 383; *Acc. Chem. Res.* **1978,** *11,* 107; c) P.S. Skell, J.J. Havel, M.J. McGlinchey, *Acc. Chem. Res.* **1973,** *6,* 97.

[9] a) G. Winkelhofer, R. Janoschek, F. Fratev, P.v.R. Schleyer, *Croat. Chem. Acta* **1983,** *56,* 509; b) R. Krishnan, M.F. Frish, J.A. Pople, P.v.R. Schleyer, *Chem. Phys. Lett.* **1981,** *79,* 408; J. Chandrasekhar, R.A. Khan, P.v.R. Schleyer, *ibid.* **1982,** *85,* 493; c) J.A. Pople, R. Krishnan, H.B. Schlegel, J.S. Binckley, *Int. J. Quant. Chem.* **1978,** *14,* 545; d) G. Frenking, *Chem. Phys. Lett.* **1983,** *100,* 484; e) P. Rosmus, P. Botschwina, J.P. Maier, *ibid.* **1981,** *84,* 71; f) C.E. Dykstra, H.F. Schaefer III, *J. Am. Chem. Soc.* **1978,** *100,* 1378; Y. Osamura, H.F. Schaefer III, S.K. Gray, W.H. Miller, *ibid.* **1981,** *103,* 1904; M.P. Conrad, H.F. Schaefer III, *ibid.* **1978,** *100,* 7820; Y. Osamura, H.F. Schaefer III, *Chem. Phys. Lett.* **1981,** *79,* 412; g) T. Carrington, Jr., L.M. Hubbard, H.F. Schaefer III, W.H. Miller, *J. Chem. Phys.* **1984,** *80,* 4347; h) A.H. Laufer, Y.L. Yung, *J. Phys. Chem.* **1983,** *87,* 181; i) K.A. White, G.C. Schatz, *ibid.* **1984,** *88,* 2049; J.H. Davies, W.A. Goddard III, L.B. Harding, *J. Am. Chem. Soc.* **1977,** *99,* 2919; j) O.P. Strausz, R.J. Norstrom, A.G. Hopkinson, M. Schoenborn, I.G. Csizmadia, *Theor. Chim. Acta* **1973,** *29,* 183; k) A.C. Scheiner, H.F. Schaefer, III, *J. Am. Chem. Soc.* **1985,** *107,* 4451.

[10] a) C. Reisen, F.M. Lussier, C.C. Jensen, J.I. Steinfeld, *J. Am. Chem. Soc.* **1979,** *101,* 350; C. Reisen, J.I. Steinfeld, *J. Phys. Chem.* **1980,** *84,* 680; b) P.S. Skell, F.A. Fargone, K.J. Klabunde, *J. Am. Chem. Soc.* **1972,** *94,* 7802; c) S.M. Burnett, A.E. Stevens, C.S. Feigerle, W.C. Lineberger, *Chem. Phys. Lett.* **1983,** *100,* 124; see also ref. 25.

[11] 'The H.M.O. Model and its Applications', Eds. E. Heilbronner and H. Bock, Wiley, London, 1976.

[12] 'Mechanism and Theory in Organic Chemistry', Eds. T.H. Lowry and K.S. Richardson, 2nd edn., Harper and Row, New York, 1981, p. 197 and ref. therein.

[13] M.H. Chisholm H.C. Clark, *J. Am. Chem. Soc.* **1972,** *94,* 1532; *Acc. Chem. Res.* **1973,** *6,* 241; M.H. Chisholm, *Platinum Met. Rev.* **1975,** *19,* 100; see also: H.C. Clark, V.K. Jain, G.S. Rao, *J. Organomet. Chem.* **1983,** *259,* 275.

[14] a) R. Hoffmann, *Angew. Chem., Int. Ed.* **1982,** *21,* 714; b) T.A. Albright, *Tetrahedron* **1982,** *38,* 1339; c) 'Orbital Interactions in Chemistry', Eds. T.A. Albright, J.K. Burdett, and M.-H. Whangbo, Wiley, New York, 1985.

[15] a) B.E.R. Schilling, R. Hoffmann, D.L. Lichtenberger, *J. Am. Chem. Soc.* **1979,** *101,* 585; b) N.M. Kostic, R.F. Fenske, *Organometallics* **1982,** *2,* 974.

[16] R. Hoffmann, J.R. Swenson, C.-C. Wan, *J. Am. Chem. Soc.* **1973,** *95,* 7644; H. Fujimoto, R. Hoffmann, *J. Phys. Chem.* **1974,** *78,* 1167.

[17] M.J.S. Dewar, *Bull. Soc. Chim. Fr.* **1951,** *18,* C79; J. Chatt, L.A. Duncanson, *J. Chem. Soc.* **1953,** 2939.

[18] B.R. Brooks, H.F. Schaefer III, *Mol. Phys.* **1977,** *197,* 1037.

[19] a) W. Ströhmeier, H. Hellmann, *Chem. Ber.* **1965,** *98,* 1598; see also: K.G. Caulton, *Coord. Chem. Rev.* **1981,** *38,* 1; b) Y. Kurima, F. Ohta, N. Ohtsuka, E. Tsuchida, *Chem. Lett.* **1983,** 1787.

[20] N.G. Bokiy, Yu.V. Gatilov, Yu.T. Struchkov, N.A. Ustynyuk, *J. Organomet. Chem.* **1973,** *54,* 213.

[21] 'Hydrocarbon Thermal Isomerizations', Ed. J.J. Gajewski, Academic Press, New York 1981, p. 15.

[22] a) H.A. Frey, *Chem. Ind.* **1960,** 1266; b) M.E. Jacox, D.E. Milligan, *J. Am. Chem. Soc.* **1963,** *85,* 278; c) N. Honjou, J. Pacansky, M. Yoshimine, *J. Am. Chem. Soc.* **1984,** *106,* 5361.

[23] a) L. Radom, P.C. Hariharan, J.A. Pople, P.v.R. Schleyer, *J. Am. Chem. Soc.* **1973,** *95,* 6531; b) K. Raghavachari, R.P. Whiteside, J.A. Pople, P.v.R. Schleyer, *ibid.* **1981,** *103,* 5649; c) 'Vinyl Cations', Eds. P.J. Stang, Z. Rappoport, M. Hanack, and L.R. Subramanian, Academic Press, New York, 1979.

[24] a) M.I. Bruce, A.G. Swincer, *Aust. J. Chem.* **1980,** *33,* 1471; b) O.M. Abu-Salah, M.I. Bruce, *J. Chem. Soc., Dalton Trans.* **1974,** 2302; c) A. Davison, J.P. Selegue, *J. Am. Chem. Soc.* **1978,** *100,* 7763; d) H. Berke, *Z. Naturforsch., B* **1980,** *35,* 86.

[25] A. Davison, J.P. Solar, *J. Organomet. Chem.* **1978,** *155,* C8; M.I. Bruce, A.G. Swincer, R.C. Wallis, *ibid.* **1979,** *171,* C5; M.I. Bruce, F.S. Wong, B.W. Skelton, A.H. White, *J. Chem. Soc., Dalton Trans.* **1982,** 2203.

[26] M. Elian, R. Hoffmann, *Inorg. Chem.* **1975,** *14,* 1058.

[27] a) R. Burt, M. Cooke, M. Green, *J. Chem. Soc. A* **1970,** 2981; b) J. Clemens, M. Green, M.C. Kuo, C.J. Fritchie, J.T. Mague, F.G.A. Stone, *Chem. Commun.* **1972,** 53; c) Y. Wakatsuki, H. Yamasaki, *Tetrahedron Lett.* **1974,** 4549; d) T. Blackmore, M.I. Bruce, F.G.A. Stone, R.E. Davis, A. Gartza, *Chem. Commun.* **1971,** 852; e) P.C. Waites, H. Weigold, A.P. Bell, *J. Organomet. Chem.* **1974,** *67,* 616; f) A.J. Hubert, J. Dale, *J. Chem. Soc.* **1965,** 3160; g) T. Funabiki, Y. Yamasaki, Y. Sato, S. Yoshida, *J. Chem. Soc., Perkins Trans. 2* **1983,** 1915; h) T. Blackmore, M.I. Bruce, F.G.A. Stone, *J. Chem. Soc., Dalton Trans.* **1974,** 106; i) E.R. Ewitt, R.G. Bergman, *J. Am. Chem. Soc.* **1980,** *100,* 7003.

[28] S. Otsuka, A. Nakamura, *Adv. Organomet. Chem.* **1976,** *14,* 245.

[29] O. Eisenstein, R. Hoffmann, *J. Am. Chem. Soc.* **1981,** *103,* 4308.

[30] P.O. Nubel, T.L. Brown, *Organometallics* **1984,** *3,* 29.

[31] R. Hoffmann, F. Beier, E.L. Muetterties, A.R. Rossi, *Inorg. Chem.* **1977,** *16,* 511.

[32] O. Bars, P. Braunstein, *Angew. Chem., Int. Ed.* **1982,** *21,* 308.

[33] L.S. Meriwether, E.C. Colthup, G.W. Kennerly, R.N. Reusch, *J. Org. Chem.* **1961,** *26,* 5155; L.S. Meriwether, M.F. Leto, E.C. Colthup, G.W. Kennerly, *ibid.* **1962,** *27,* 3930.

[34] a) Y. Tohda, K. Sonogashira, N. Hagihara, *J. Chem. Soc., Chem. Commun.* **1975,** 54; b) J. Grobe, B.H. Schneider, H. Zimmerman *Z. Naturforsch., B* **1984,** *39,* 957.

[35] a) J. Wolf, H. Werner, O. Serhadli, M.L. Ziegler, *Angew. Chem.* **1983,** *95,* 428; *ibid. Int. Ed.* **1983,** *22,* 414; b) H. Werner, H. Otto, T. Ngo-Khac, C. Burschka, *J. Organomet. Chem.* **1984,** *262,* 123; M.I. Bruce, R.C.F. Gardner, J.A.K. Howard, F.G.A. Stone, M. Welling, P. Woodward, *J. Chem. Soc., Dalton Trans.* **1977,** 621.

[36] a) K. Mueller, *Angew. Chem., Int. Ed.* **1980,** *19,* 1; b) L. Salem, 'Electrons in Chemical Reactions', J. Wiley, New York, 1982.

[37] H. Werner, personal communication.

[38] D.R. Saunders, R.J. Mawby, *J. Chem. Soc., Chem. Commun.* **1984,** 140; *J. Chem. Soc., Dalton Trans.* **1984,** 2133; for another recent example of this type of reaction: J.T. Gauntlett, R.F. Taylor, M.J. Winter, *Chem. Commun.* **1984,** 421.

[39] H. Berke, R. Hoffmann, *J. Am. Chem. Soc.* **1978,** *100,* 7224.

[40] a) W.R. Roper, L.J. Wright, *J. Organomet. Chem.* **1977,** *142,* C1; b) G. Fachinetti, C. Floriani, A. Rosetti, S. Pucci, *J. Chem. Soc., Chem. Commun.* **1978,** 269; c) G. Fachinetti, C. Floriani, H. Stoeckli-Evans, *ibid.* **1977,** 2297; d) W.R. Roper, G.E. Taylor, J.M. Water, L.J. Wright, *J. Organomet. Chem.* **1979,** *182,* C46; e) P.J. Fajan, J.M. Manriquez, T.J. Marks, V.W. Day, S.H. Vollmer, C.S. Day, *J. Am. Chem. Soc.* **1980,** *102,* 5396; f) C.D. Wood, R.R. Schrock, *J. Am. Chem. Soc.* **1979,** *101,* 5421.

[41] K.L. Brown, G.L. Clark, C.E.L. Headford, K. Marschen, W.R. Roper, *J. Am. Chem. Soc.* **1979,** *101,* 503.

[42] J.X. Dermott, M.E. Wilson, G.M. Whitesides, *J. Am. Chem. Soc.* **1976,** *98,* 6529; G. Fachinetti, C. Floriani, *J. Chem. Soc., Chem. Commun.* **1972,** 654; H. Masai, K. Sonogashira, N. Hagihara, *Bull. Chem. Soc. Jpn.* **1968,** *41,* 750; E. Carmona-Guzman, G. Wilkinson, *J. Chem. Soc., Dalton Trans.* **1978,** 1139.

[43] N.E. Kolobova, V.V. Skripkin, T.V. Rozantsera, Yu.T. Struchkov, G.G. Aleksandrov, V.A. Antonovich, V.I. Bakhmutov, *Koord. Khim.* **1982,** *8,* 1655.

[44] a) D.M. Hoffman, R. Hoffmann, C.R. Fisel, *J. Am. Chem. Soc.* **1982,** *104,* 3858; b) D.M. Hoffman, R. Hoffmann, *J. Chem. Soc., Dalton Trans.* **1982,** 1471.

[45] Y. Koie, S. Sinoda, Y. Saito, B.J. Fitzgerald, C.G. Pierpont, *Inorg. Chem.* **1980,** *19,* 770.

[46] A.N. Nesmeyanov, A.B. Antonova, N.E. Kolobova, K.N. Anisimov, *Izv. Akad. Nauk. SSSR, Ser. Khim.* **1974,** 2873; A.N. Nesmeyanov, N.E. Kolobova, A.B. Antonova, K.N. Anisimov, *Dokl. Akad. Nauk, SSSR* **1975,** *220,* 105; L.N. Lewis, J.C. Huffman, K.G. Caulton, *J. Am. Chem. Soc.* **1980,** *102,* 403; N.E. Kolobova, T.V. Rozantsera, P.V. Petrovskii, *Izv. Akad. Nauk. SSSR, Ser. Khim.* **1979,** 2063; N.E. Kolobova, L.L. Ivanov, O.S. Zhvanko, P.V. Petrovskii, *ibid.* **1981,** 432.

[47] G. Trinquier, R. Hoffmann, *Organometallics* **1984,** *3,* 370.

[48] J.G. Hamilton, J.J. Rooney, *J. Chem. Soc., Faraday Trans. 1* **1984,** *80,* 129.

[49] a) 'Principles and Applications of Organotransition Metal Chemistry', Eds. J.P. Collman, and L.S. Hegedus; University Science Books, Mill Valley, 1980; b) G. Muller, to be published; c) J.M. Huggins, R.G. Bergman, *J. Am. Chem. Soc.* **1981,** *103,* 3002 and ref. therein.

[50] a) D. Afzal, P.G. Lenhert, C.M. Lukehart, *J. Am. Chem. Soc.* **1984,** *106,* 3050; b) T.G. Attig, H.C. Clark, C.S. Wong, *Can. J. Chem.* **1977,** *55,* 189.

[51] J.R. Shapley, S.J. Richter, M. Tachikawa, J.B. Keister, *J. Organomet. Chem.* **1975,** *94,* C43; A.D. Clauss, M. Tachikawa, J.R. Shapley, C.G. Pierpont, *Inorg. Chem.* **1981,** *20,* 1578.

[52] P.O. Nubel, T.L. Brown, *J. Am. Chem. Soc.* **1984,** *106,* 644, 3474.

[53] M. Green, A.G. Orpen, C.J. Schaverien, *J. Chem. Soc., Chem. Commun.* **1984,** 37.

[54] a) E.L. Muetterties, T.N. Rhodin, E. Band, C.F. Brucker, W.F. Pretzer, *Chem. Rev.* **1979,** *79,* 91; b) E.L. Muetterties, *J. Organomet. Chem.* **1980,** *200,* 177; c) E.L. Muetterties, *Bull. Soc. Chim. Belg.* **1976,** *85,* 451; *ibid.* **1975,** *84,* 959.

[55] D.R. Lloyd, F.P. Netzer, *Surf. Sci.* **1983,** *129,* L249; R.J. Koestner, M.A. Van Hove, G.A. Somorjai, *J. Phys. Chem.* **1983,** *87,* 203; *Chem. Tech.* **1983,** *13,* 376.

[56] a) 'Transition Metal Clusters', Ed. B.F.G. Johnson, J. Wiley, New York, 1980; b) 'Mechanisms of Inorganic and Organometallic Reactions', Ed. M.V. Twigg, Plenum Press, New York, 1983; c) E. Sappa, A. Tiripicchio, P. Braunstein, *Chem. Rev.* **1983,** *83,* 203; d) A.P. Humphries, H.D. Kaesz, *Progr. Inorg. Chem.* **1978,** *25,* 145; e) A.A. Koridze, O.A. Kizas, N.E. Kolobova, P.V. Petrovskii, *Akad. Nauk, SSSR* **1984,** 472.

[57] B.E.R. Schilling, R. Hoffmann, *J. Am. Chem. Soc.* **1979,** *101,* 3456.

[58] E. Sappa, O. Gambino, L. Milone, G. Cetini, *J. Organomet. Chem.* **1972,** *39,* 169.

[59] A.J. Carty, *Pure Appl. Chem.* **1982,** *54,* 113.

[60] a) A.J. Deeming, M. Underhill, *J. Chem. Soc., Dalton Trans.* **1973,** 277; R.D. Adams, D.A. Katahira, L.-W. Yang, *Organometallics* **1982,** *1,* 235; b) A.J. Deeming, I.P. Rothwell, M.B. Hursthouse, J.D.J. Backer-Dircks, *J. Chem. Soc., Dalton Trans.* **1981,** 1879; c) A.J. Deeming, S. Hasso, M. Underhill, *ibid.* **1975,** 1614.

[61] C.J. Cooksey, A.J. Deeming, I.P. Rothwell, *J. Chem. Soc., Dalton Trans.* **1981,** 1718.

[62] M.A. Andrews, H.D. Kaesz, *J. Am. Chem. Soc.* **1979,** *101,* 7238.

[63] M.A. Andrews, G. Van Buskirk, C.B. Knobler, H.D. Kaesz, *J. Am. Chem. Soc.* **1979,** *101,* 7245.

[64] H.D. Kaesz, personal communication.

[65] M. Laing, P. Sommerville, Z. Dawoodi, M.J. Mays, P.J. Wheatley, *J. Chem. Soc., Chem. Commun.* **1978,** 1035.

[66] M.R. Churchill, B.G. De Boer, *Inorg. Chem.* **1977,** *16,* 878.

[67] R.L. Burch, A.I. Schusterman, E.L. Muetterties, R.G. Teller, J.M. Williams, *J. Am. Chem. Soc.* **1983,** *105,* 3546.

[68] a) S. Aime, L. Milone, E. Sappa, A. Tiripicchio, *J. Chem. Soc., Dalton Trans.* **1977,** 227; b) S. Aime, G. Gervasio, L. Milone, E. Sappa, M. Franchini Angela, *Inorg. Chim. Acta* **1978,** *26,* 223; c) V. Raverdino, S. Aime, L. Milone, E. Sappa, *ibid.* **1978,** *30,* 9; d) E. Sappa, A. Tiripicchio, M. Tiripicchio Camellini, *J. Chem. Soc., Chem. Commun.* **1979,** 254; e) E. Sappa, A.M. Manotti Lanfredi, A. Tiripicchio, *J. Organomet. Chem.* **1981,** *221,* 93; f) M. Castiglioni, R. Giordano, E. Sappa, *ibid.* **1983,** *258,* 217.

[69] R. Hoffmann, *J. Chem. Phys.* **1963,** *34,* 1397; R. Hoffmann, W.N. Lipscomb, *ibid.* **1962,** *36,* 3179, 3489; *ibid.* **1962,** *37,* 2872.

[70] J.H. Ammeter, H.-B. Bürgi, J.C. Thibeault, R. Hoffmann, *J. Am. Chem. Soc.* **1978,** *100,* 3686; R. Hoffmann, P. Hoffmann, *ibid.* **1976,** *98,* 598.

[71] T.A. Albright, R. Hoffmann, *Chem. Ber.* **1978,** *111,* 1578.

[72] D.L. Du Bois, R. Hoffmann, *Nouv. J. Chim.* **1977,** *1,* 479.